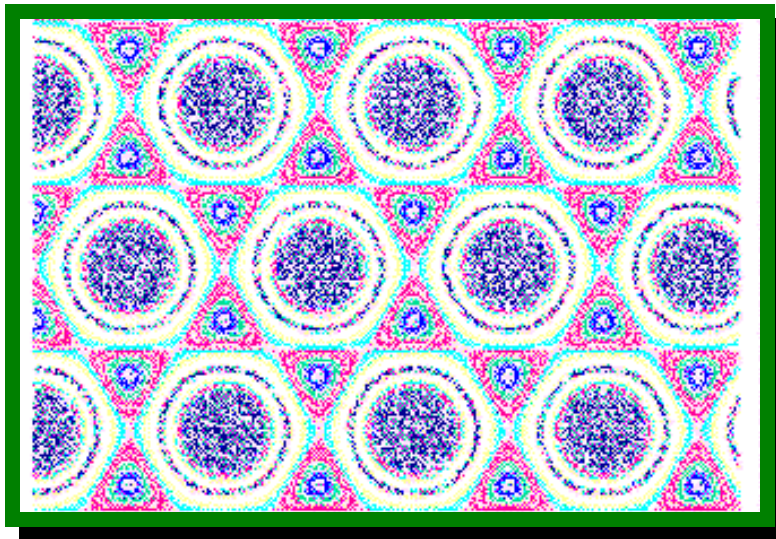


Superconductivity The Structure Scale of the Universe

Seventh Edition
August 01, 2005

Richard D. Saam P.E.

Proteus Systems Inc.
525 Louisiana Ave
Corpus Christi, Texas 78404 USA
e-mail: rdsaam@att.net



ABSTRACT

A theoretical framework supported by experimental evidence is presented which indicates that superconductivity is a relativistic phenomenon and congruent with the concept of a Bose Einstein Condensate and Charge Conjugation, Parity Change and Time Reversal (CPT) theorem. A momentum and energy conserving (elastic) CPT lattice and associated superconducting theory is postulated whereby electromagnetic and gravitational forces are mediated by a particle of relativistic velocity transformed mass (m_t) ($110.123 \times$ electron mass) and unit charge congruent with Heisenberg Uncertainty, such that the established electron/proton mass is maintained, electron and proton charge is maintained and the universe radius is $2.25E28$ cm, the universe mass is $3.02E56$ gram, the universe density is $6.38E-30$ g/cm³ or $2/3$ the critical density. The universe time or age is $1.37E10$ years and the universe Hubble constant is $2.31E-18$ /sec (71.2 km/sec-million parsec). The calculated universe mass and density are based on an isotropic homogeneous media filling the vacuum of space analogous to the 'aether' referred to in the 19th century (but still in conformance with Einstein's relativity theory) and could be considered a candidate for the 'dark matter/energy' in present universe theories. Each particle of mass m_t in the proposed dark matter has a volume of 15733 cm³. In this context the universe cosmic microwave background radiation (CMBR) black body temperature is linked to universe dark matter/energy superconducting temperature. The model predicts an acceleration value with observed universe expansion and consistent with observed Pioneer 10 & 11 deep space translational and rotational deceleration. Also, a reasonable value for the cosmological constant is derived having dimensions of the known universe. Also, a YBCO superconductor should lose .04% of its weight while 100% in superconducting mode which is close to reported results by Podkletnov and Nieminen (.05%). All of this is placed in context of the virial theorem. Also this trisine model predicts 1, 2 and 3 dimensional superconductors which has been verified by observed magnesium diboride (MgB₂) superconductor critical data. Also dimensional guidelines are provided for design of room temperature superconductors and beyond and which are related to practical goals such as fabricating a superconductor with the energy content equivalent to the combustion energy of gasoline. These dimensional guidelines have been experimentally verified by Homes' Law and generally fit the parameters of a superconductor operating in the "dirty" limit.

PREVIOUS PUBLICATION

First Edition October 15, 1996
<http://xxx.lanl.gov/abs/physics/9705007>
Title: Superconductivity, the Structure Scale of the Universe
Author: Richard D. Saam
Comments: 61 pages, 27 references, 11 figures
(.pdf available on request) from rdsaam@att.net
Subj-class: General Physics

Second Edition May 1, 1999
<http://xxx.lanl.gov/abs/physics/9905007>, version 6
Title: Superconductivity, the Structure Scale of the Universe
Author: Richard D. Saam
Comments: 61 pages, 27 references, 16 tables, 16 figures,
Subj-class: General Physics

Third Edition February 23, 2002
<http://xxx.lanl.gov/abs/physics/9905007>, version 7
Title: Superconductivity, the Structure Scale of the Universe
Author: Richard D. Saam
Comments: 66 pages, 50 references, 27 tables, 17 figures
Subj-class: General Physics

Fourth Edition February 23, 2005
<http://xxx.lanl.gov/abs/physics/9905007>, version 9
Title: Superconductivity, the Structure Scale of the Universe
Author: Richard D. Saam
Comments: 46 columnated pages, 21 figures, 17 tables, 192 equations, 58 references
Subj-class: General Physics

Fifth Edition April 15, 2005
<http://xxx.lanl.gov/abs/physics/9905007>, version 11
Title: Superconductivity, the Structure Scale of the Universe
Author: Richard D. Saam
Comments: 46 columnated pages, 21 figures, 17 tables, 192 equations, 58 references
Subj-class: General Physics

Sixth Edition June 01, 2005
<http://xxx.lanl.gov/abs/physics/9905007>, version 13
Title: Superconductivity, the Structure Scale of the Universe
Author: Richard D. Saam
Comments: 47 columnated pages, 21 figures, 17 tables, 192 equations, 63 references
Subj-class: General Physics

Copyright © 1996, 1999, 2002, 2005 Proteus Systems Inc.

All rights reserved.

Reference of this material is encouraged.

TABLE OF CONTENTS

- 1. INTRODUCTION**
 - 2. TRISINE MODEL DEVELOPMENT**
 - 2.1 DEFINING MODEL RELATIONSHIPS**
 - 2.2 TRISINE GEOMETRY**
 - 2.3 TRISINE CHARACTERISTIC WAVE VECTORS**
 - 2.4 TRISINE CHARACTERISTIC DE BROGLIE VELOCITIES AND SAGNAC RELATIONSHIP**
 - 2.5 SUPERCONDUCTOR DIELECTRIC CONSTANT AND MAGNETIC PERMEABILITY**
 - 2.6 FLUXOID AND CRITICAL FIELDS**
 - 2.7 SUPERCONDUCTOR INTERNAL PRESSURE, CASIMIR FORCE AND DEEP SPACE DRAG FORCE (PIONEER 10 & 11)**
 - 2.8 SUPERCONDUCTING CURRENT, VOLTAGE AND CONDUCTANCE (AND HOMES' LAW)**
 - 2.9 SUPERCONDUCTOR WEIGHT REDUCTION IN A GRAVITATIONAL FIELD**
 - 2.10 BCS VERIFYING CONSTANTS**
 - 2.11 SUPERCONDUCTING COSMOLOGICAL CONSTANT**
 - 2.12 SUPERCONDUCTING VARIANCE AT T/T_c**
 - 2.13 SUPERCONDUCTOR ENERGY CONTENT**
 - 2.14 SUPERCONDUCTOR GRAVITATIONAL ENERGY**
 - 3. DISCUSSION**
 - 4. CONCLUSION**
 - 5. VARIABLE AND CONSTANT DEFINITIONS**
- APPENDICES**
- A. TRISINE NUMBER AND B/A RATIO DERIVATION**
 - B. DEBYE MODEL NORMAL AND TRISINE RECIPROCAL LATTICE WAVE VECTORS**
 - C. ONE DIMENSION AND TRISINE DENSITY OF STATES**
 - D. GINZBURG-LANDAU EQUATION AND TRISINE STRUCTURE RELATIONSHIP**
 - E. LORENTZ EINSTEIN TRANSFORMATION CONSEQUENCE**
- 6. REFERENCES**

1. INTRODUCTION

Trisine structure is a model for superconductivity based on Gaussian surfaces surrounding superconducting Cooper CPT Charge conjugated pairs. This Gaussian surface has the same configuration as a particular matrix geometry as defined in reference [1], and essentially consists of mirror image non parallel surface pairs. The main purpose of the lattice has and is to control the flow of particles suspended in a fluid stream and generally has been fabricated on a macroscopic scale. In this particular configuration, a lattice is described wherein there is a perfect elasticity to fluid flow. In other words there is 100 percent conservation of energy and momentum which by definition we will assume to describe the phenomenon of superconductivity.

The superconducting model presented herein is a logical translation of this geometry in terms of classical and quantum theory to provide a basis for explaining aspects of the superconducting phenomenon and integration of this phenomenon with gravitational forces within the context of references[1-63].

This approach is an attempt to articulate a geometrical model for superconductivity in order to anticipate dimensional regimes in which one could look for higher performance materials. This approach does not address specific particles such as polarons, excitons, magnons, plasmons which may be necessary for the expression of superconductivity in a given material. Indeed, the Trisine structure or lattice as presented in this report may be expressed in terms of something more profound and elementary and that is the Charge Conjugate Parity Change Time Reversal (CPT) Theorem.

Superconductivity is keyed to a critical temperature(T_c) which is representative of the energy at which the superconductive property takes place in a material. The material that is characterized as a superconductor has this property at all temperatures below the critical temperature.

In terms of the trisine model, any critical temperature can be inserted, but for the purposes of this report, six critical temperatures are selected as follows:

$$1.1 \quad T_c \quad 8.11E-16^\circ K \quad T_b \quad 2.729^\circ K$$

The background temperature of the Universe represented by the black body cosmic microwave background radiation (CMBR) of $2.728 \pm .004^\circ K$ as detected in all directions of space in 60 - 630 GHz frequency range by the FIRAS instrument in the Cobe satellite and $2.730 \pm .014^\circ K$ as measured at 10.7 GHz from a balloon platform [26]. The most recent

NASA estimation of CMBR temperature is $2.725 \pm .002^\circ K$. The particular temperature of $2.729^\circ K$ indicated above which is essentially equal to the CMBR temperature was established by the trisine model wherein the superconducting Cooper CPT Charge conjugated pair density (see table 2.9.1) ($6.38E-30 \text{ g/cm}^3$) equals the density of the universe (see equation 2.11.5).

$$1.2 \quad T_c \quad 93^\circ K \quad T_b \quad 7.05E8^\circ K$$

The critical temperature of the $YBa_2Cu_3O_{7-x}$ superconductor as discovered by Paul Chu at the University of Houston and which was the basis for the gravitational shielding effect of .05% as observed by Podkletnov and Nieminen(see Table 2.9.1).

$$1.3 \quad T_c \quad 447^\circ K \quad T_b \quad 1.55E9^\circ K$$

The critical temperature of an anticipated room temperature superconductor which is calculated to be 1.5×298 degree Kelvin such that the superconducting material may have substantial superconducting properties at an operating temperature of 298 degree Kelvin.

$$1.4 \quad T_c \quad 1190^\circ K \quad T_b \quad 2.52E9^\circ K$$

The critical temperature of an anticipated material which would have an energy content equivalent to the combustion energy content of gasoline(see Table 2.13.1).

$$1.5 \quad T_c \quad 2,135^\circ K \quad T_b \quad 3.23E9^\circ K$$

The critical temperature of an anticipated superconducting material with the assumed density (6.39 g/cm^3) [17] of $YBa_2Cu_3O_{7-x}$ which would generate its own gravity to the extent that it would be weightless in earth's gravitational field (See Table 2.9.1).

$$1.6 \quad T_c \quad 3,100,000^\circ K \quad T_b \quad 1.29E11^\circ K$$

The upper bounds of the superconductive phenomenon as dictated by relativistic effects wherein material dielectric equals one (See Table 2.5.1).

As a general comment, a superconductor should be operated at about $2/3$ of (T_c) for maximum effect of most properties which are usually expressed as when extrapolated to $T = 0$

(see section 2.12). In this light, critical temperatures (T_c) in items 1.4 & 1.5 could be operated up to 2/3 of the indicated temperature (793 and 1300 degree Kelvin respectively) and still retain superconducting properties characteristic of the indicated (T_c). Also, the present development is for one dimensional superconductivity. Consideration should be given to 2 and 3 dimensional superconductivity by 2 or 3 multiplier to T_c 's contained herein interpret experimental results.

2. TRISINE MODEL DEVELOPMENT

In this report, mathematical relationships which link trisine geometry and superconducting theory are developed and then numerical values are presented in accordance with these relationships. Centimeter, gram and second(cgs) as well as Kelvin temperature units are used unless otherwise specified. The actual model is developed in spread sheet format with all model equations computed simultaneously and interactively as required.

2.1 DEFINING MODEL RELATIONSHIPS

The four defining model equations are presented as 2.1.1 - 2.1.4 below:

$$\iint d(\text{Area}) = 4\pi(\text{Cooper } e_{\pm}) \quad (2.1.1)$$

$$\begin{aligned} \frac{2m_t k_b T_c}{\hbar^2} &= \frac{(KK)}{e^{\text{trisine}} - 1} \\ &= \frac{e^{\text{Euler}} (KK)}{\pi \sinh(\text{trisine})} \\ &= K_B^2 \end{aligned} \quad (2.1.2)$$

$$\text{trisine} = \frac{1}{D(\epsilon_t) \cdot V} \quad (2.1.3)$$

$$f\left(\frac{m_t}{m_e}\right) \frac{e_{\pm} \hbar}{2m_e v_{\epsilon}} = \text{cavity } H_c \quad (2.1.4)$$

Equation 2.1.1 is a representation of Gauss's law with a

Cooper CPT Charge conjugated pair charge contained within a bounding surface area. Equation 2.1.2 and 2.1.3 define the superconducting model as developed by Bardeen, Cooper and Schrieffer in references [2] and Kittel in in references [4].

The objective is then to select a particular (*wave vector*)^c or $(KK)_{\text{how}}$ based on trisine geometry (see figures 2.2.1-2.2.5) that fits the model relationship as indicated in equation 2.1.2 with K_B^2 being defined as the trisine (*wave vector*)^z or (KK) associated with superconductivity of Cooper CPT Charge conjugated pairs through the lattice. This procedure establishes the trisine geometrical dimensions, then equation 2.1.4 is used to establish an effective mass function $f(m_t/m_e)$ of the particles in order for particles to flip in spin when going from trisine *cavity* to *cavity* while in thermodynamic equilibrium with critical field H_c . As a check on this method, conservation of momentum p and energy E are assumed such that:

$$\sum_{n=1,2,3,4} \Delta p_n \Delta x_n = 0 \quad (2.1.5)$$

$$K_1 + K_2 \rightleftharpoons K_3 + K_4$$

(conservation of momentum)

$$\sum_{n=1,2,3,4} \Delta E_n \Delta t_n = 0 \quad (2.1.6)$$

$$K_1 K_1 + K_2 K_2 \rightleftharpoons K_3 K_3 + K_4 K_4$$

(conservation of energy)

These conditions of conservation of momentum and energy provide the necessary condition of perfect elasticity which must exist in the superconducting state. In addition, the superconducting state may be viewed as boiling of states $\Delta E_n, \Delta t_n, \Delta p_n, \Delta x_n$ on top of the zero point state in a coordinated manner.

The trisine symmetry (as visually seen in figures 2.2.1-2.2.5) allows movement of Cooper CPT Charge conjugated pairs with center of mass wave vector equal to zero as required by superconductor theory as presented in references [2, 4].

Wave vectors (K) as applied to trisine are assumed to be free particles (ones moving in the absence of any potential field) and are solutions to the one dimensional Schrödinger equation [3]:

$$\frac{d^2 \psi}{ds^2} + \frac{2m_t}{\hbar^2} \text{Energy } \psi = 0 \quad (2.1.7)$$

The well known solution to the one dimensional Schrödinger equation is in terms of a wave function(ψ) is:

$$\begin{aligned} \psi &= \text{Amplitude} \sin\left(\left(\frac{2m_t}{\hbar^2} \text{Energy}\right)^{\frac{1}{2}} s\right) \\ &= \text{Amplitude} \sin(K \cdot s) \end{aligned} \quad (2.1.8)$$

Wave vector solutions (KK) are constrained to fixed trisine cell boundaries such that energy eigen values are established by the condition $s = S$ and $\psi = 0$ such that

$$\left(\frac{2m_t}{\hbar^2} \text{Energy}\right)^{\frac{1}{2}} S = K S = n\pi \quad (2.1.9)$$

Energy eigen values are then described in terms of what is generally called the particle in the box relationship as follows:

$$\text{Energy} = \frac{n^2 \hbar^2}{2m_t} \left(\frac{\pi}{S}\right)^2 \quad (2.1.10)$$

For our model development, we assume the quantum number $n = 2$ and this quantum number is incorporated into the wave vectors (KK) as presented as follows:

$$\begin{aligned} \text{Energy} &= \frac{2^2 \hbar^2}{2m_t} \left(\frac{\pi}{S}\right)^2 \\ &= \frac{\hbar^2}{2m_t} \left(\frac{2\pi}{S}\right)^2 \\ &= \frac{\hbar^2}{2m_t} (KK) \end{aligned} \quad (2.1.11)$$

Trisine geometry is described in Figure 1-5 is in general characterized by relativistic dimensions A and B with a characteristic ratio B/A of 2.37933 and corresponding characteristic angle(θ) where:

$$\theta = \tan^{-1}\left(\frac{A}{B}\right) = \tan^{-1}\left(\frac{1}{e} \frac{2}{\sqrt{3}}\right) = 22.80^\circ \quad (2.1.12)$$

The superconducting model is described with equations 2.1.13 - 2.1.16, with variable definitions described in the remaining equations. The model essentially falls within the concept of a Bose Einstein Condensate (BEC). The model converges around a particular relativistic velocity transformed mass (m_t) (110.123 x electron mass(m_e)) and dimensional ratio(B/A) of 2.37855.

$$\begin{aligned} k_b T_c &= \left\{ \begin{array}{l} \frac{\hbar^2 K_B^2}{2m_t} \\ \frac{\hbar^2 (K_C^2 + K_{Ds}^2)}{2m_t} \frac{1}{e^{\text{trisine}} - 1} \\ \frac{\hbar^2 (K_C^2 + K_{Ds}^2)}{2m_t} \frac{e^{\text{Euler}}}{\pi \sinh(\text{trisine})} \\ \frac{\hbar^2}{\frac{m_e m_t}{m_e + m_t} (2B)^2 + \frac{m_t m_p}{m_t + m_p} (A)^2} \\ \left(\frac{1}{g_s^2}\right) \frac{\text{cavity}}{8\pi} DE \\ \frac{1}{g_s^3} \frac{\text{chain}}{\text{cavity}} \frac{e_{\pm}^2}{\epsilon B} \\ \frac{2\pi \hbar}{\text{time}} \end{array} \right\} \quad (2.1.13) \\ &= \frac{m_t v_{dx}^2}{2} = \frac{1}{2} \hbar \omega \end{aligned}$$

BCS theory is adhered to as verified by equation 2.1.13, array element 3 in conjunction with equations A.3, A.4, and A.5 as derived in Appendix A. Also, Bose Einstein Condensate criteria is satisfied as:

$$\text{cavity}^{\frac{1}{3}} = \frac{h}{\sqrt{2\pi m_t k_b T}} \quad (2.1.13a)$$

$$\begin{aligned} \text{trisine} &= \frac{K_B^2 + K_P^2}{K_P K_B} \\ &= \frac{1}{D(\epsilon) V} \\ &= -\ln\left(\frac{2}{\pi} e^{\text{Euler}} - 1\right) \end{aligned} \quad (2.1.14)$$

$$\text{density of states } D(\epsilon_T) = \frac{3 \text{ cavity } m_t K_C}{4\pi^3 \hbar^2} \quad (2.1.15)$$

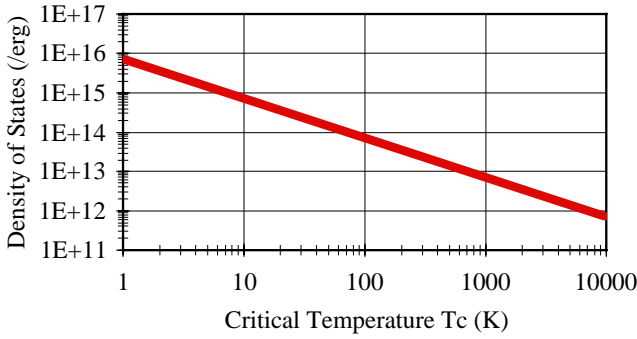
$$= \frac{1}{k_b T_c}$$

The attractive Cooper CPT Charge conjugated pair energy (V) is:

$$V = \frac{K_p K_B}{K_B^2 + K_p^2} k_b T_c \quad (2.1.16)$$

Table 2.1.1 with Density of States (/erg) Plot

$T_c (^{\circ}K)$	3,100,000	2,135	1,190	447	93	8.11E-16
$T_b (^{\circ}K)$	1.29E+11	3.38E+09	2.52E+09	1.55E+09	7.05E+08	2.729
V (erg)	2.12E-10	1.46E-13	8.13E-14	3.05E-14	6.35E-15	5.54E-32
$D(\epsilon)$ (/erg)	2.34E+09	3.39E+12	6.09E+12	1.62E+13	7.79E+13	8.93E+30



The equation 2.1.13 array element 2 and 3 along with equations 2.1.14, 2.1.15, 2.1.16, 2.1.17 and 2.1.18 are consistent with the BCS weak link relationship:

$$k_b T_c = \frac{2e^{Euler}}{\pi} \frac{\hbar^2}{2m_t} (K_C^2 + K_{Ds}^2) e^{\frac{-1}{D(\epsilon)V}} \quad (2.1.17)$$

$$k_b T_c = \left(\frac{1}{g_s}\right) \left(\frac{chain}{cavity}\right) \frac{\hbar^2}{2m_t} \left(\frac{K_A^2}{C}\right) e^{\frac{-1}{D(\epsilon)V}} \quad (2.1.18)$$

The relationship in equation 2.1.19 is based on the Bohr magneton $e\hbar/2m_e v_e$ (which has dimensions of magnetic field x volume) with a material dielectric (ϵ) modified speed of light (v_e) and establishes the spin flip/flop as Cooper CPT Charge conjugated pairs go from one cavity to the next (see figure 2.3.1). The 1/2 spin factor and electron gyromagnetic factor (g_e) and superconducting gyro factor (g_s) are multipliers of the Bohr magneton where $g_s = (m_t/(m_t - m_e))(m_p/(m_p - m_e))$ as related to the

Dirac Number by $(3/4)(g_s - 1) = 2\pi(g_d - 1)$. Also because particles must advance in pairs, a symmetry is created for superconducting current to advance as bosons.

$$\frac{1}{2} g_e g_s \frac{m_t}{m_e} \frac{e\hbar}{2m_e v_e} = \text{cavity } H_c \quad (2.1.19)$$

Proton to electron mass ratio (m_p/m_e) is verified through the Werner Heisenberg Uncertainty Principle volume ($\Delta x \cdot \Delta y \cdot \Delta z$) as follows:

$$\left\{ \begin{array}{l} \Delta x \\ \Delta y \\ \Delta z \end{array} \right\} = \left\{ \begin{array}{l} \frac{\hbar}{2 \Delta p_x} \\ \frac{\hbar}{2 \Delta p_y} \\ \frac{\hbar}{2 \Delta p_z} \end{array} \right\} = \left\{ \begin{array}{l} \frac{\hbar}{2 \Delta (\hbar K_B)} \\ \frac{\hbar}{2 \Delta (\hbar K_P)} \\ \frac{\hbar}{2 \Delta (\hbar K_A)} \end{array} \right\} \left\{ \begin{array}{l} \Delta \left(\frac{B}{2\pi} \right) \\ \Delta \left(\frac{3B}{2\sqrt{3}} \frac{1}{2\pi} \right) \\ \Delta \left(\frac{A}{2} \frac{1}{2\pi} \right) \end{array} \right\} \quad (2.1.20)$$

$$(\Delta x \cdot \Delta y \cdot \Delta z) = \frac{1}{(2K_B)(2K_P)(2K_A)} \quad (2.1.21)$$

$$\frac{m_p}{m_e} = \frac{m_t - m_e}{m_t + m_e} \frac{\text{cavity}}{(\Delta x \Delta y \Delta z)} - \frac{m_t + 2m_e}{m_e} \quad (2.1.22)$$

Equations 2.1.20 - 2.1.22 provides us with the confidence ($\Delta x \cdot \Delta y \cdot \Delta z$ is well contained within the *cavity*) that we can proceed in a semi-classical manner outside the envelop of the uncertainty principle with the relativistic velocity transformed mass (m_t) and De Broglie velocities (v_d) used in this trisine superconductor model or in other words equation 2.1.23 holds.

$$\mathbb{C} \left(\frac{\hbar^2 (KK)}{2m_t} \right) = \mathbb{C} \left(\frac{1}{2} m_t v_d^2 \right) \quad (2.1.23)$$

$$= \frac{(m_t v_d)^2}{m_t}$$

The Meissner condition as defined by total magnetic field exclusion from trisine chain as indicated by diamagnetic susceptibility (X) = $-1/4\pi$, is adhered to by the following equation:

$$X = -\frac{\mathbb{C} k_b T_c}{chain H_c^2} = -\frac{1}{4\pi} \quad (2.1.24)$$

Equation 2.1.25 provides a representation of the relativistic

velocity transformed mass (m_t)

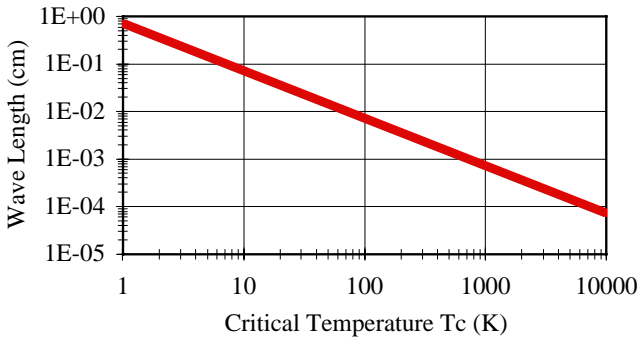
$$\frac{m_t v_d^2}{2c^2} \frac{1}{1 - \sqrt{1 - \frac{v_d^2}{c^2}}} = m_r \frac{1}{1 - \sqrt{1 - \frac{v_d^2}{c^2}}} \quad (2.1.25)$$

$$= m_t$$

where $v_d \ll c$

Table 2.1.2 with Wave Length (cm) Plot

T_c ($^{\circ}K$)	3,100,000	2,135	1,190	447	93	8.11E-16
T_s ($^{\circ}K$)	1.29E+11	3.38E+09	2.52E+09	1.55E+09	7.05E+08	2.729
m_t (g)	1.00E-25	1.00E-25	1.00E-25	1.00E-25	1.00E-25	1.00E-25
m_r (g)	4.76E-31	3.28E-34	1.83E-34	6.87E-35	1.43E-35	1.25E-52
Frequency (Hz)	8.12E+17	5.59E+14	3.12E+14	1.17E+14	2.44E+13	2.12E-04
Wave length (cm)	2.32E-07	3.37E-04	6.05E-04	1.61E-03	7.74E-03	8.87E+14



Equation 2.1.25 is in conformance with the conventionally held principle that the photon rest mass equals zero.

The relativistic nature of the superconducting phenomenon is again demonstrated by equation 2.1.26 which relates the classical electron radius (R_{ce}) (2.818E-13 cm) to a relativistic length we shall call B. The velocity (v_e) is a speed of light dependent on the permittivity and permeability properties of the particular medium studied.

$$B = 6 \cdot R_{ce} \cdot \frac{m_t}{m_e} \cdot \frac{1}{1 - \sqrt{1 - \frac{v_e^2}{c^2}}} = 6 \cdot \frac{e^2}{m_e c^2} \cdot \frac{m_t}{m_e} \cdot \frac{1}{1 - \sqrt{1 - \frac{v_e^2}{c^2}}} \quad (2.1.26)$$

where $v_e \ll c$

Also a relativistic CPT $time_{\pm}$ is defined in terms of the

classical electron radius (R_{ce}) divided by the speed of light (c) or $time_{\pm}$ interval of 9.400E-24 sec.

$$time = 4 \cdot \frac{R_{ce}}{c} \cdot \frac{1}{1 - \sqrt{1 - \frac{v_d^2}{c^2}}} = 4 \cdot \frac{e_{\pm}^2}{m_e c^2} \cdot \frac{1}{c} \cdot \frac{1}{1 - \sqrt{1 - \frac{v_d^2}{c^2}}} \quad (2.1.27)$$

where $v_d \ll c$

Where (v_d) is the De Broglie velocity as in equation 2.1.28 and also related to relativistic CPT $time_{\pm}$ by equation 2.1.29.

$$v_d = \frac{\hbar \pi}{m_t B} \quad (2.1.28)$$

$$time = \frac{2 \cdot B}{v_d} \quad (2.1.29)$$

Also a relationship among zero point base energy ($\hbar\omega/2$), De Broglie velocity, relativistic CPT $time_{\pm}$, speed of light and relativistic mass is presented in equation 2.1.30.

$$energy = m_t \int \frac{v_d dv_d}{\sqrt{1 - \frac{v_d^2}{c^2}}} = m_t c^2 \left(1 - \sqrt{1 - \frac{v_d^2}{c^2}} \right) = \frac{1}{2} \cdot \hbar \cdot \omega \cdot \frac{1}{1 - \sqrt{1 - \frac{v_d^2}{c^2}}} = \frac{1}{2} \cdot \hbar \cdot \frac{2\pi}{time} \cdot \frac{1}{1 - \sqrt{1 - \frac{v_d^2}{c^2}}} = \frac{1}{2} \cdot m_t \cdot v_d^2 \cdot \frac{1}{1 - \sqrt{1 - \frac{v_d^2}{c^2}}} \quad (2.1.30)$$

where $v_d \ll c$

Conceptually, it is though the electron radius and $time_{\pm}$ were spread out or dilated to the *trisine* dimensions. Lorentz Einstein transformations are in accordance with Appendix E.

The relationship between (v_{dx}) and (v_{ex}) is per the group/phase velocity relationship presented in equation 2.1.31.

$$(\text{group velocity}) \cdot (\text{phase velocity}) = c^2$$

$$(v_{dx}) \cdot \left(\frac{1}{\pi} \frac{v_{\epsilon x}^2}{v_{dx}^2} \cdot c \right) = (v_{dx}) \cdot \left(\frac{1}{\frac{B}{A} 3^{\frac{1}{4}} v_{dx}^2} \cdot c \right) \quad (2.1.31)$$

$$= c^2$$

2.2 TRISINE GEOMETRY

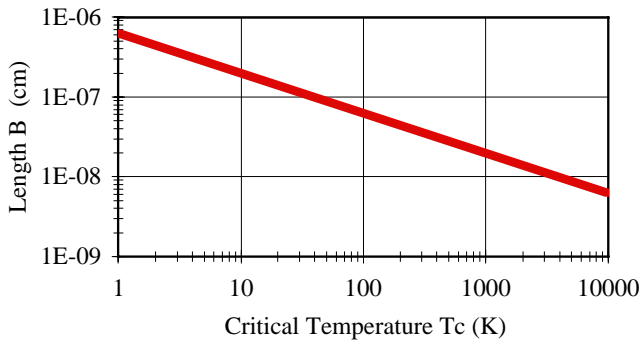
The characteristic trisine relativistic dimensions A and B are indicated as a function of temperature in table 2.2.1 as computed from the equation 2.2.1

$$k_b T_c = \frac{\hbar^2 K_B^2}{2m_t} = \frac{\hbar^2 K_A^2}{2m_t} \left(\frac{B}{A} \right)^2 \quad (2.2.1)$$

Trisine Geometry is subject to Charge conjugation Parity change Time reversal (CPT) -symmetry which is a fundamental symmetry of physical laws under transformations that involve the inversions of charge , parity and time simultaneously.

Table 2.2.1 with B vs Tc plot

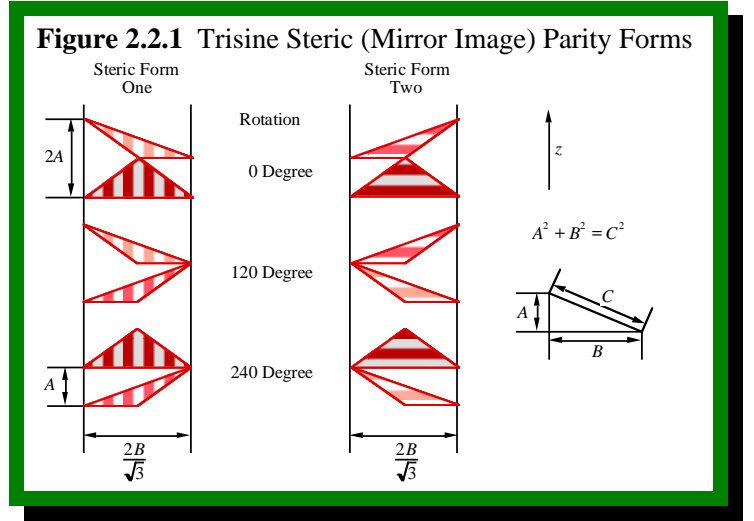
$T_c (^{\circ}K)$	3,100,000	2,135	1,190	447	93	8.11E-16
$T_s (^{\circ}K)$	1.29E+11	3.38E+09	2.52E+09	1.55E+09	7.05E+08	2.729
A (cm)	1.50E-10	5.73E-09	7.67E-09	1.25E-08	2.74E-08	9.29
B (cm)	3.58E-10	1.36E-08	1.82E-08	2.98E-08	6.53E-08	22.11



$$A = \frac{2 e^{Euler}}{\pi} \frac{3 e_{\pm}^2}{m_e c^2} \frac{1}{1 - \sqrt{1 - \frac{v_{\epsilon y}^2}{c^2}}} \quad (2.2.2)$$

$$= \frac{e_{\pm}}{time_{\pm} \cdot H_c \cdot v_{\epsilon x}} \frac{m_t}{m_e} \quad \left(\begin{array}{l} \text{Biot-Savart} \\ \text{eqn 2.6.3} \end{array} \right)$$

$$B = g_s \frac{6 e_{\pm}^2}{m_e c^2} \frac{1}{1 - \sqrt{1 - \frac{v_{\epsilon x}^2}{c^2}}} \quad (2.2.3)$$



Trisine characteristic volumes with variable names *cavity* and *chain* as well as characteristic areas with variable names *section*, *approach* and *side* are defined in equations 2.2.2 - 2.2.6. See figures 2.2.1 - 2.2.4 for a visual description of these parameters. The mirror image forms in figure 2.2.1 are in conformance with parity requirement in Charge conjugation Parity change Time reversal (CPT) theorem as established by determinant identity in equation 2.2.3a.

$$\begin{vmatrix} -B & 0 & 0 \\ 0 & \frac{B}{\sqrt{3}} & -\frac{B}{\sqrt{3}} \\ -\frac{A}{2} & 0 & \frac{A}{2} \end{vmatrix} = - \begin{vmatrix} 0 & 0 & B \\ 0 & \frac{B}{\sqrt{3}} & -\frac{B}{\sqrt{3}} \\ -\frac{A}{2} & 0 & \frac{A}{2} \end{vmatrix} \quad (2.2.3a)$$

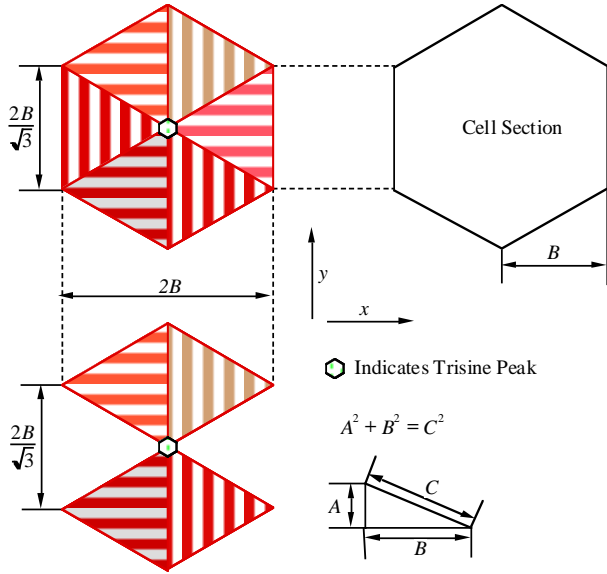
$$cavity = 2\sqrt{3}AB^2 \quad (2.2.4)$$

$$chain = \frac{2}{3}cavity \quad (2.2.5)$$

The *section* is the trisine cell *cavity* projection on to the *x, y* plane as indicated in figure 2.2.2.

$$section = 2\sqrt{3}B^2 \quad (2.2.6)$$

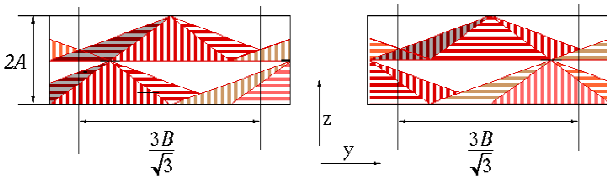
Figure 2.2.2 Trisine Cavity and Chain Geometry from Steric (Mirror Image) Forms



The *approach* is the trisine cell *cavity* projection on to the y, z plane as indicated in figure 2.2.3.

$$\text{approach} = \frac{1}{2} \frac{3B}{\sqrt{3}} 2A = \sqrt{3}AB \quad (2.2.7)$$

Figure 2.2.3 Trisine *approach* from both *cavity* approaches



The *side* is the trisine cell *cavity* projection on to the x, z plane as indicated in figure 2.2.4.

$$\text{side} = \frac{1}{2} 2A \cdot 2B = 2AB \quad (2.2.8)$$

Figure 2.2.4 Trisine *side* view from both *cavity* sides

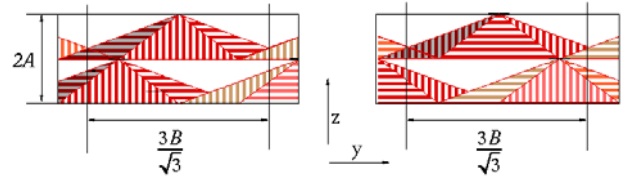


Table 2.2.2 with cavity and section plots

T_c ($^{\circ}K$)	3,100,000	2,135	1,190	447	93	8.11E-16
T_b ($^{\circ}K$)	1.29E+11	3.38E+09	2.52E+09	1.55E+09	7.05E+08	2.729
Cavity (cm^3)	6.65E-29	3.68E-24	8.85E-24	3.84E-23	4.05E-22	15733
chain (cm^3)	4.44E-29	2.45E-24	5.90E-24	2.56E-23	2.70E-22	10489
section (cm^2)	4.43E-19	6.43E-16	1.15E-15	3.07E-15	1.48E-14	1693
approach (cm^2)	9.31E-20	1.35E-16	2.42E-16	6.45E-16	3.10E-15	356
side (cm^2)	1.07E-19	1.56E-16	2.80E-16	7.45E-16	3.58E-15	411

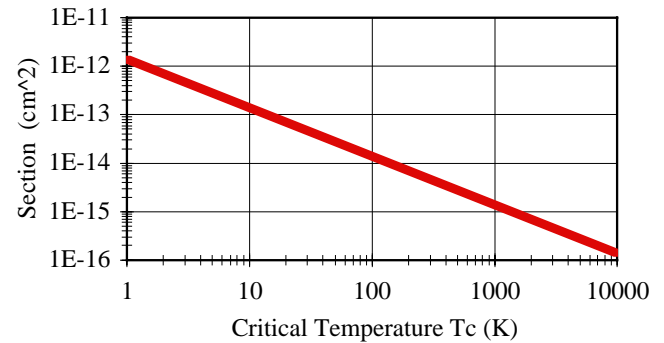
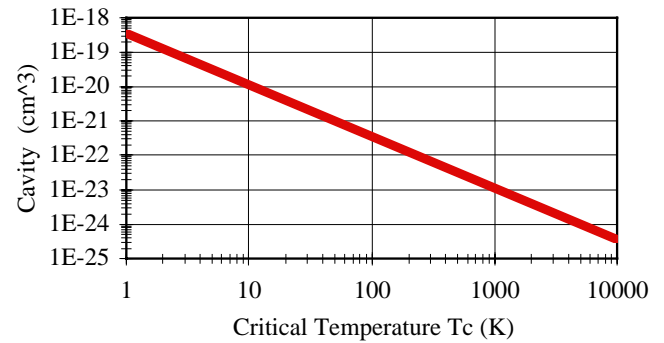
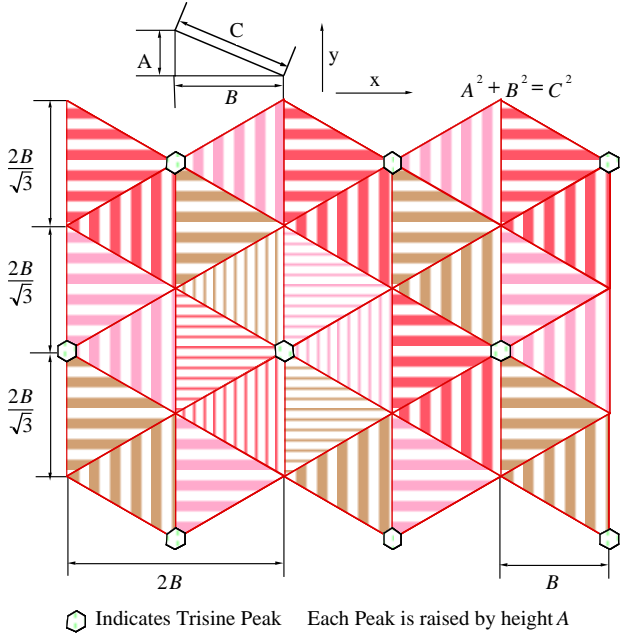


Figure 2.2.5 Trisine Geometry

2.3 TRISINE CHARACTERISTIC WAVE VECTORS

Superconducting model trisine characteristic wave vectors K_{Dn} , K_{Ds} and K_C are defined in equations 2.3.1 - 2.3.3 below.

$$K_{Dn} = \left(\frac{6\pi^2}{\text{cavity}} \right)^{\frac{1}{3}} \quad (2.3.1)$$

The relationship in equation 2.3.1 represents the normal Debye wave vector (K_{Dn}) assuming the *cavity* volume conforming to a sphere in K space and also defined in terms of K_A , K_P and K_B as defined in equations 2.3.4, 2.3.5 and 2.3.6.

See Appendix B for the derivation of equation 2.3.1.

$$K_{Ds} = \left(\frac{8\pi^3}{\text{cavity}} \right)^{\frac{1}{3}} = (K_A K_B K_P)^{\frac{1}{3}} \quad (2.3.2)$$

The relationship in equation 2.3.2 represents the normal Debye wave vector (K_{Ds}) assuming the *cavity* volume conforming to a characteristic trisine cell in K space.

See Appendix B for the derivation of equation 2.3.2.

$$K_C = \frac{4\pi}{3\sqrt{3}A} \quad (2.3.3)$$

The relationship in equation 2.3.3 represents the result of equating one dimensional and trisine density of states.

See Appendix C for the derivation of equation 2.3.3.

Equations 2.3.4, 2.3.5, and 2.3.6 translate the trisine wave vectors K_C , K_{Ds} , and K_{Dn} into x, y, z Cartesian coordinates as represented by K_B , K_P , and K_A respectively. The superconducting current is in the x direction.

$$K_B = \left(\frac{1}{g_s} \right) (K_{Dn} + K_{Ds}) - K_C = \frac{2\pi}{2B} \quad (2.3.4)$$

$$K_P = g_s (K_{Dn} - K_{Ds}) + K_C = \frac{2\pi\sqrt{3}}{3B} \quad (2.3.5)$$

$$K_A = g_s^4 (K_{Ds}) + K_{Dn} + K_C = \frac{2\pi}{A} \quad (2.3.6)$$

Note that the energy relationships of wave vectors are as follows:

$$K_A^2 > K_C^2 > K_{Ds}^2 > K_P^2 > K_B^2 \quad (2.3.7)$$

Equation 2.3.8 relates addition of wave function amplitudes $(B/\sqrt{3})$, $(P/2)$, $(B/2)$ in terms of superconducting energy ($k_b T_c$).

$$k_b T_c = \frac{\text{cavity } \hbar}{\text{chain time}_\pm} \left(\begin{array}{l} + \frac{K_B}{2B} \left(\frac{B}{\sqrt{3}} \right)^2 \\ + \frac{K_P}{2P} \left(\frac{P}{2} \right)^2 \\ + \frac{K_A}{2A} \left(\frac{A}{2} \right)^2 \end{array} \right) \quad (2.3.8)$$

The wave vector K_B , being the lowest energy, is the carrier of the superconducting energy and in accordance with derivation in appendix A. All of the other wave vectors are contained within the cell *cavity*.

$$\frac{m_e m_t}{m_e + m_t} \frac{1}{K_B^2} + \frac{m_t m_p}{m_t + m_p} \frac{1}{K_A^2} = \frac{1}{6} g_s^2 m_t \frac{1}{K_C^2} \quad (2.3.9)$$

$$K_C = \frac{1}{g_s} \frac{2\pi}{\sqrt{A^2 + B^2}} \quad (2.3.10)$$

The conservation of momentum and energy relationships in 2.3.11 and 2.3.12 are dictated and verified by the B/A ratio of 2.37933.

$$\sum_{n=B,C,Ds,Dn} \Delta p_n \Delta x_n = 0 \quad (2.3.11)$$

$$g_s (K_B + K_C) \rightleftharpoons K_{Ds} + K_{Dn}$$

(conservation of momentum)

$$\sum_{n=B,C,Ds,Dn} \Delta E_n \Delta t_n = 0 \quad (2.3.12)$$

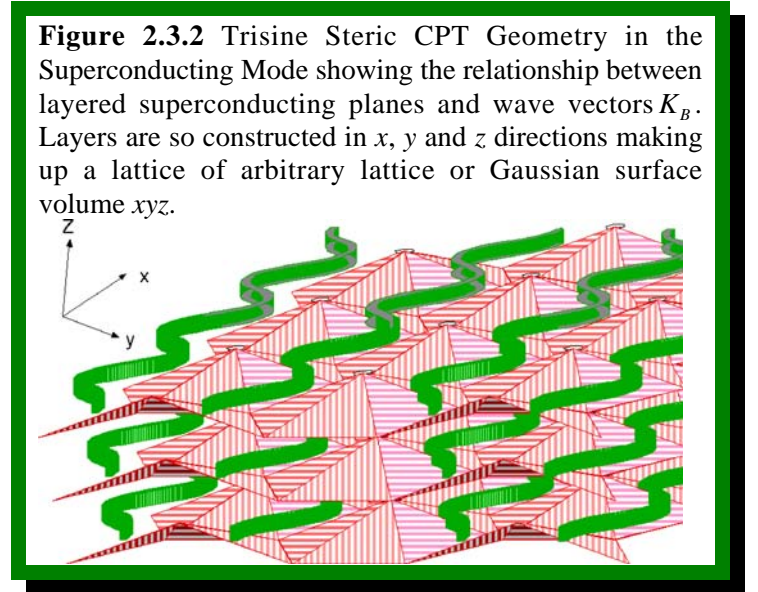
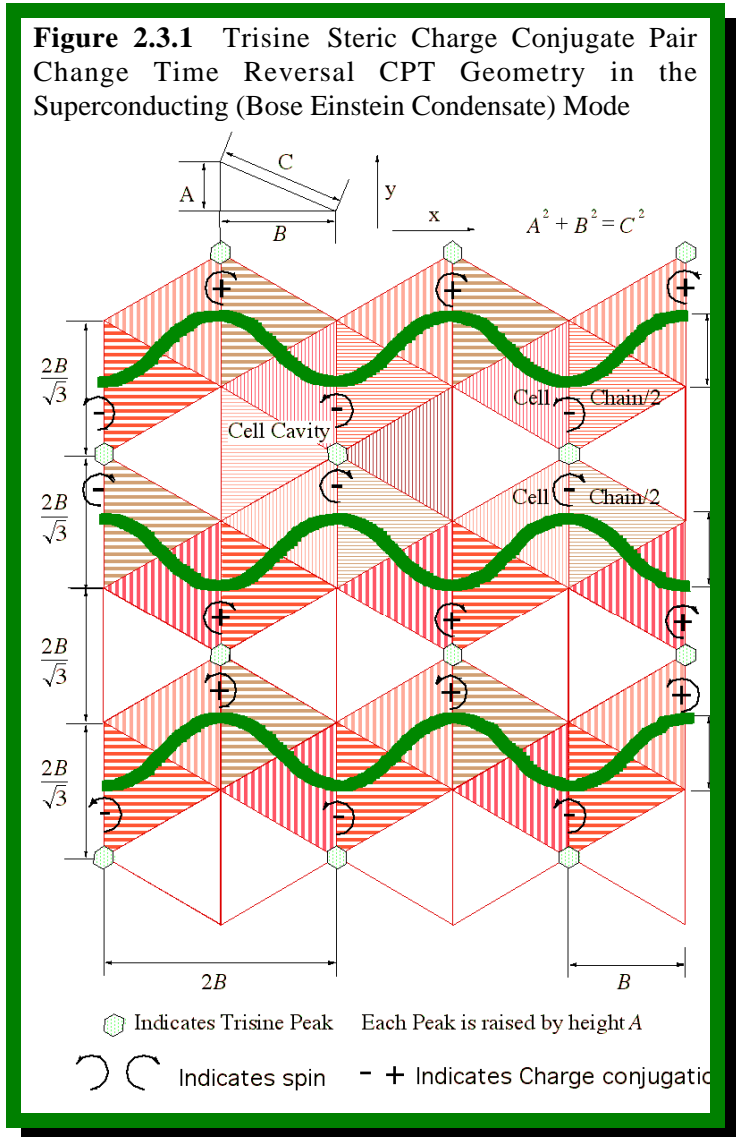
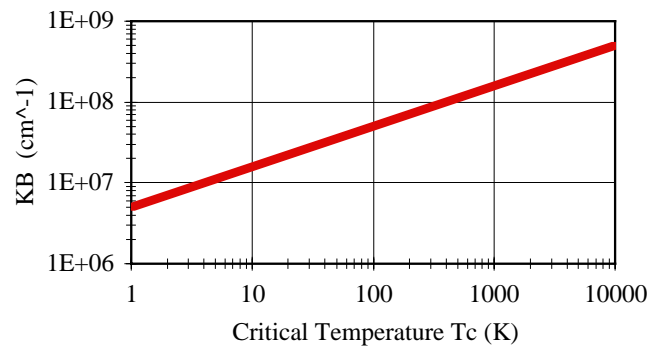
$$K_B^2 + K_C^2 \rightleftharpoons g_s (K_{Ds}^2 + K_{Dn}^2)$$

(conservation of energy)

with the Charge conjugation Parity change Time reversal (CPT) theorem. Negative and positive charge reversal as well as time reversal take place in mirror image parity pairs.

Table 2.3.1 with K_B Plot

$T_c (^{\circ}K)$	3,100,000	2,135	1,190	447	93	8.11E-16
$T_s (^{\circ}K)$	1.29E+11	3.38E+09	2.52E+09	1.55E+09	7.05E+08	2.729
$K_B (/cm)$	8.79E+09	2.31E+08	1.72E+08	1.06E+08	4.81E+07	1.42E-01
$K_{Dn} (/cm)$	9.62E+09	2.52E+08	1.88E+08	1.16E+08	5.27E+07	1.56E-01
$K_{Ds} (/cm)$	1.55E+10	4.07E+08	3.04E+08	1.86E+08	8.49E+07	2.51E-01
$K_C (/cm)$	1.61E+10	4.22E+08	3.15E+08	1.93E+08	8.82E+07	2.60E-01
$K_p (/cm)$	1.02E+10	2.67E+08	1.99E+08	1.22E+08	5.56E+07	1.64E-01
$K_A (/cm)$	4.18E+10	1.10E+09	8.19E+08	5.02E+08	2.29E+08	6.76E-01



2.4 TRISINE CHARACTERISTIC DE BROGLIE VELOCITIES

Figure 2.3.1 in conjunction with mirror image parity images in Figure 2.2.1 clearly depict the trisine symmetry congruent

The Cartesian De Broglie velocities (v_{dx}) , (v_{dy}) , and (v_{dz}) as well as (v_{dc}) are computed with the trisine Cooper CPT Charge conjugated pair residence *relativistic CPT time*_± and

characteristic frequency(ω) in phase with trisine superconducting dimension($2B$) in equations 2.4.1-2.4.5.

$$v_{dx} = \frac{\hbar K_B}{m_t} = \frac{2B}{time_{\pm}} = \frac{\omega}{2\pi} 2B = \frac{eH_c}{m_e v_{\epsilon}} g_s^6 B \quad (2.4.1)$$

In equation 2.4.1, note that $m_e v_{\epsilon} / eH_c$ is the electron spin axis precession rate in the critical magnetic field(H_c). This electron spin rate is in tune with the electron moving with De Broglie velocity(v_{dx}) with a CPT residence $time_{\pm}$ in each cavity. In other words the Cooper CPT Charge conjugated pair flip spin twice per cavity and because each Cooper CPT Charge conjugated pair flips simultaneously, the quantum is an $2(1/2)$ or integer which corresponds to a boson.

$$v_{dy} = \frac{\hbar K_P}{m_t} \quad (2.4.2)$$

$$v_{dz} = \frac{\hbar K_A}{m_t} \quad (2.4.3)$$

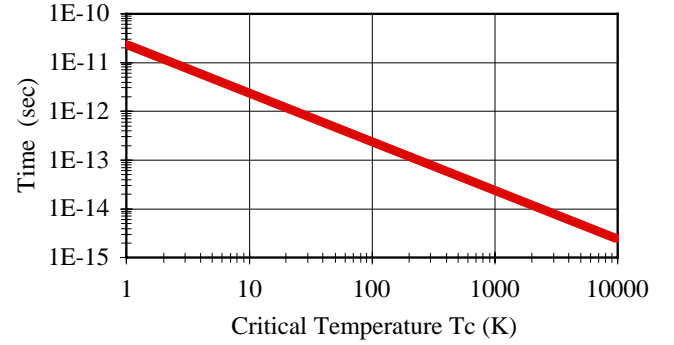
$$v_{dC} = \frac{\hbar K_C}{m_t} \quad (2.4.4)$$

The vector sum of the x , y , z and C De Broglie velocity components are used to compute a three dimensional helical or tangential De Broglie velocity(v_{dT}) as follows:

$$\begin{aligned} v_{dT} &= \sqrt{v_{dx}^2 + v_{dy}^2 + v_{dz}^2} \\ &= \frac{\hbar}{m_t} \sqrt{K_A^2 + K_B^2 + K_P^2} \\ &= \frac{3}{g_s} \cos(\theta) v_{dC} \end{aligned} \quad (2.4.5)$$

Table 2.4.1 Listing of De Broglie velocities, trisine cell pair residence relativistic CPT time $_{\pm}$ and characteristic frequency(ω) as a function of selected critical temperature(T_c) and Debye black body temperature(T_b) along with a time $_{\pm}$ plot.

T_c ($^{\circ}K$)	3,100,000	2,135	1,190	447	93	8.11E-16
T_b ($^{\circ}K$)	1.29E+11	3.38E+09	2.52E+09	1.55E+09	7.05E+08	2.729
v_{dx} (cm/sec)	9.24E+07	2.42E+06	1.81E+06	1.11E+06	5.06E+05	1.49E-03
v_{dy} (cm/sec)	1.07E+08	2.80E+06	2.09E+06	1.28E+06	5.84E+05	1.72E-03
v_{dz} (cm/sec)	4.40E+08	1.15E+07	8.61E+06	5.28E+06	2.41E+06	7.11E-03
v_{dC} (cm/sec)	1.69E+08	4.44E+06	3.31E+06	2.03E+06	9.27E+05	2.74E-03
v_{dT} (cm/sec)	4.62E+08	1.21E+07	9.05E+06	5.54E+06	2.53E+06	7.47E-03
Time $_{\pm}$ (sec)	7.74E-18	1.12E-14	2.02E-14	5.37E-14	2.58E-13	2.96E+04
ω (/sec)	8.12E+17	5.59E+14	3.12E+14	1.17E+14	2.44E+13	2.12E-04



Equation 2.4.6 represents a check on the trisine cell residence relativistic CPT time $_{\pm}$ as computed from the precession of each electron in a Cooper CPT Charge conjugated pair under the influence of the perpendicular critical field(H_c). Note that the precession is based on the electron mass(m_e) and not trisine relativistic velocity transformed mass(m_t).

$$time_{\pm} = \frac{1}{g_s^6} \frac{m_e v_{\epsilon}}{e_{\pm} H_c B} \quad (2.4.6)$$

Another check on the trisine cell residence relativistic CPT time $_{\pm}$ is computed on the position of the Cooper CPT Charge conjugated pair($C e$) particles under the charge influence of each other within the dielectric(ϵ) as they travel in the y direction as expressed in equation 2.4.7.

$$m_t \frac{d^2 y}{dt^2} = \frac{M_a e_{\pm}^2}{\epsilon \cos(\theta)} \frac{1}{y^2} \quad (2.4.7)$$

From figure 2.3.1 it is seen that the Cooper CPT Charge conjugated pairs travel over distance $(3B/\sqrt{3} - 2B/\sqrt{3})$ in

each quarter cycle or *relativistic CPT time*_±/4.

$$time_{\pm} = 4 \left(\frac{8}{81} \frac{m_t \varepsilon \cos(\theta)}{M_a e_{\pm}^2} \right)^{\frac{1}{2}} \left(\frac{3B}{\sqrt{3}} - \frac{2B}{\sqrt{3}} \right)^{\frac{3}{2}} \quad (2.4.8)$$

where the Madelung constant (M_y) in the y direction is calculated as:

$$M_y = \sqrt{3} \sum_{n=0}^{n=\infty} \left(\frac{1}{3(1+2n)-1} - \frac{1}{3(1+2n)+1} \right) \quad (2.4.9)$$

$$= 0.523598679$$

And the Thomas scattering formula[43] holds in terms of the following equation:

$$Side = \left(\frac{K_B}{K_{Ds}} \right) \left(\frac{8\pi}{3} \right) \left(\frac{e_{\pm}^2}{M_y \varepsilon m_t v_{dy}^2} \right)^2 \quad (2.4.10)$$

A sense of the rotational character of the De Broglie (v_{dT}) velocity can be attained by the following energy equation:

$$\frac{1}{2} m_t v_{dT}^2 = \frac{1}{g_s} \cos(\theta) \frac{chain}{cavity} \frac{1}{2} (m_t (2B)^2) \omega^2 \quad (2.4.11)$$

$$+ \frac{1}{g_s} \cos(\theta) \frac{chain}{cavity} \frac{1}{2} (m_t (A)^2) \omega^2$$

Equation 2.4.12 provides an expression for the Sagnac time.

$$time_{\pm} = \frac{\sqrt{A^2 + B^2}}{B} \frac{2\pi}{time_{\pm}} \frac{section}{6} \frac{1}{v_{dx}^2} \quad (2.4.12)$$

2.5 SUPERCONDUCTOR DIELECTRIC CONSTANT AND MAGNETIC PERMEABILITY

The material dielectric is computed by determining a displacement (D) (equation 2.5.1) and electric field (E) (equation 2.5.2) and which establishes a dielectric (ε or D/E) (equation 2.5.3) and modified speed of light (v_{ε} or $c/\sqrt{\varepsilon}$) (equation 2.5.4). Then the superconducting fluxoid (Φ_{ε}) (equation 2.5.5) can be calculated.

The electric field (E) is calculated by taking the translational energy ($m_t v_{dx}^2/2$) (which is equivalent to $k_b T_c$) over a distance which is the trisine cell volume to surface ratio. This concept

of the surface to volume ratio is used extensively in fluid mechanics for computing energies of fluids passing through various geometric forms and is called the hydraulic ratio.

$$E = \left(\frac{1}{g_s^2} \right) \left(\mathbb{C} \frac{m_t v_{dx}^2}{2} \right) \left(\frac{2 \text{ section}}{\cos(\theta)} \right) \left(\frac{1}{\mathbb{C} e_{\pm} \text{ cavity}} \right) \quad (2.5.1)$$

$$= 4.25 \frac{1}{2} \frac{m_t v_{dx}^2}{\mathbb{C} e_{\pm} A}$$

Secondarily, the electric field (E) is calculated in terms of the forces ($m_t v_d / time$) exerted by the wave vectors (K).

$$E = \left\{ \begin{array}{l} 10 \left(g_s^2 \frac{m_t v_{dx} \cos(\theta)}{time_{\pm}} \right) \left(\frac{1}{\mathbb{C} e_{\pm}} \right) \\ 9 \left(\frac{1}{g_s^2} \frac{m_t v_{dy}}{time_{\pm}} \right) \left(\frac{1}{\mathbb{C} e_{\pm}} \right) \\ 2 \left(\frac{1}{g_s} \frac{1}{\cos(\theta)} \frac{m_t v_{dz}}{time_{\pm}} \right) \left(\frac{1}{\mathbb{C} e_{\pm}} \right) \\ 6 \left(\frac{m_t v_{dc} \cos(\theta)}{time_{\pm}} \right) \left(\frac{1}{\mathbb{C} e_{\pm}} \right) \end{array} \right. \quad (2.5.2)$$

The trisine cell surface is ($section/\cos(\theta)$) and the volume is expressed as *cavity*. Note that the trisine *cavity*, although bounded by ($2 \cdot section / \cos(\theta)$), still has the passageways for Cooper CPT Charge conjugated pairs (Ce) to move from cell *cavity* to cell *cavity*.

The displacement (D) as a measure of Gaussian surface containing free charges ($\mathbb{C} e_{\pm}$) is computed by taking the (4π) solid angle divided by the characteristic trisine area ($section/\cos(\theta)$) with the two(2) charges ($\mathbb{C} e_{\pm}$) contained therein and in accordance with Gauss's law as expressed in equation 2.1.1.

$$D = 4\pi \mathbb{C} e_{\pm} \frac{\cos(\theta)}{2 \text{ section}} \quad (2.5.3)$$

Now a dielectric coefficient can be calculated from the electric field (E) and displacement field (D) [61].

$$\varepsilon = \frac{D}{E} \quad (2.5.4)$$

Assuming the trisine geometry has the relative magnetic permeability of a vacuum ($k_m = 1$) then a modified velocity of light (v_ϵ) can be computed from the dielectric coefficient (ϵ) and the speed of light (c) where ($\epsilon_0 = 1$).

$$v_\epsilon = \frac{c}{\sqrt{k_m \frac{\epsilon}{\epsilon_0}}} = \frac{c}{\sqrt{\epsilon}} \quad (2.5.5)$$

Trisine incident/reflective angle (Figure 2.3.1) of 30 degrees is less than Brewster angle of $\tan^{-1}(\epsilon/\epsilon) = 45^\circ$ assuring total reflectivity as particles travel from trisine lattice cell to trisine lattice cell.

Now the fluxoid (Φ_ϵ) can be computed quantized according to (*Cooper e*) as experimentally observed in superconductors.

$$\Phi_\epsilon = \frac{2\pi\hbar v_\epsilon}{\mathbb{C} e_\pm} \quad (2.5.6)$$

Table 2.5.1 with dielectric plot

T_c ($^\circ K$)	3,100,000	2,135	1,190	447	93	8.11E-16
T_b ($^\circ K$)	1.29E+11	3.38E+09	2.52E+09	1.55E+09	7.05E+08	2.729
D (erg/e/cm)	1.26E+10	8.65E+06	4.82E+06	1.81E+06	3.77E+05	3.29E-12
E (erg/e/cm)	1.26E+10	2.28E+05	9.49E+04	2.18E+04	2.07E+03	5.34E-23
E (volt/cm)	3.79E+12	6.84E+07	2.85E+07	6.55E+06	6.22E+05	1.60E-20
ϵ	1.00	37.95	50.83	82.93	181.82	6.16E+10
v_ϵ (cm/sec)	3.00E+10	4.87E+09	4.21E+09	3.29E+09	2.22E+09	1.21E+05
Φ_ϵ (gauss cm ²)	2.07E-07	3.36E-08	2.90E-08	2.27E-08	1.53E-08	8.33E-13

Using the computed dielectric, the energy associated with superconductivity can be calculated in terms of the standard Coulomb's law electrostatic relationship $e^z/(\epsilon B)$ as presented in equation 2.5.7.

$$k_b T_c = \left\{ \begin{array}{l} \frac{\text{chain } e_\pm^2}{\text{cavity } \epsilon B} \\ g_s \frac{1}{\cos(\theta)} M_y \frac{\text{chain } e_\pm^2 \sqrt{3}}{\text{cavity } \epsilon B} \\ \frac{1}{g_s} \tan(\theta) \frac{\text{chain } e_\pm^2}{\text{cavity } \epsilon A} \end{array} \right\} \quad (2.5.7)$$

where M_a is the Madelung constant in y direction as computed in equation 2.4.9.

A conversion between superconducting temperature and black

body temperature is calculated in equation 2.5.9. Two primary energy related factors are involved, the first being the superconducting velocity (v_{dx}^z) to light velocity (v_ϵ^z) and the second is normal Debye wave vector (K_{Dn}^z) to superconducting Debye wave vector (K_{Ds}^z) all of this followed by a minor rotational factor for each factor involving (m_e) and (m_p). For reference, a value of 2.71 degrees Kelvin is used for the universe black body temperature (T_b) as indicated by experimentally observed microwave radiation by the Cosmic Background Explorer (COBE) and later satellites. Although the observed minor fluctuations (1 part in 100,000) in this universe background radiation indicative of clumps of matter forming shortly after the big bang, for the purposes of this report we will assume that the experimentally observed uniform radiation is indicative of present universe that is isotropic and homogeneous.

Verification of equation 2.5.6 is indicated by the calculation that superconducting density (m_i/cavity) (table 2.9.1) and present universe density (equation 2.11.4) are equal at this Debye black body temperature (T_b) of $2.71^\circ K$.

$$T_b = \frac{1}{\mathbb{C}} \left(\frac{v_\epsilon}{v_{dx}} \right)^2 g_s^3 T_c \quad (2.5.8)$$

$$k_b T_b = 2\pi\hbar \frac{c}{\lambda_b} \quad (2.5.9)$$

The black body temperatures (T_b) appear to be high relative to superconducting (T_c), but when the corresponding wave length (λ_b) is calculated in accordance with equation 2.5.7, it is nearly the same and just within the Heisenberg (Δz) parameter for all T_c and T_b as calculated from equation 2.1.18 and presented in table 2.5.2. It is suggested that a black body oscillator exists within such a volume as defined by ($\Delta x \Delta y \Delta z$) and is the source of the microwave radiation at $2.71^\circ K$. It is apparent that the high black body temperatures indicated for the other higher critical superconducting temperatures are not expressed external to the superconducting material. Could it be that the reason we observe the $2.71^\circ K$ radiation is because we as observers are inside the universe as a superconductor?

Table 2.5.2 based on equations 2.1.20 and 2.5.9

$T_c (^{\circ}K)$	3,100,000	2,135	1,190	447	93	8.11E-16
$T_b (^{\circ}K)$	1.29E+11	3.38E+09	2.52E+09	1.55E+09	7.05E+08	2.729
Δx (cm)	5.69E-11	2.17E-09	2.90E-09	4.74E-09	1.04E-08	3.52
Δy (cm)	4.93E-11	1.88E-09	2.52E-09	4.10E-09	9.00E-09	3.05
Δz (cm)	1.20E-11	4.56E-10	6.10E-10	9.96E-10	2.18E-09	0.74
λ_b (cm)	8.58E-12	3.27E-10	4.38E-10	7.15E-10	1.57E-09	0.53

Based on the same approach as presented in equations 2.5.1, 2.5.2 and 2.5.3, Cartesian x, y, and z values for electric and displacement fields are presented in equations 2.5.10 and 2.5.11.

$$\left. \begin{matrix} E_x \\ E_y \\ E_z \end{matrix} \right\} = \left\{ \begin{matrix} \frac{F_x}{\mathbb{C} e_{\pm}} \\ \frac{F_y}{\mathbb{C} e_{\pm}} \\ \frac{F_z}{\mathbb{C} e_{\pm}} \end{matrix} \right\} = \left\{ \begin{matrix} \frac{m_t v_{dx}}{time_{\pm}} \frac{1}{\mathbb{C} e_{\pm}} \\ \frac{m_t v_{dy}}{time_{\pm}} \frac{1}{\mathbb{C} e_{\pm}} \\ \frac{m_t v_{dz}}{time_{\pm}} \frac{1}{\mathbb{C} e_{\pm}} \end{matrix} \right\} \quad (2.5.10)$$

$$\left. \begin{matrix} D_x \\ D_y \\ D_z \end{matrix} \right\} = \left\{ \begin{matrix} \frac{4\pi}{\text{approach}} \mathbb{C} e_{\pm} \\ \frac{4\pi}{\text{side}} \mathbb{C} e_{\pm} \\ \frac{4\pi}{\text{section}} \mathbb{C} e_{\pm} \end{matrix} \right\} \quad (2.5.11)$$

Now assume that the superconductor material magnetic permeability (k_m) is defined as per equation 2.5.12 noting that $k_m = k_{mx} = k_{my} = k_{mz}$.

$$k_m = \left\{ \begin{matrix} k_{mx} \\ k_{my} \\ k_{mz} \end{matrix} \right\} = \left\{ \begin{matrix} \frac{D_x v_{\epsilon x}^2 E_x}{E_x D_x v_{dx}^2} \\ \frac{D_y v_{\epsilon y}^2 E_y}{E_y D_y v_{dy}^2} \\ \frac{D_z v_{\epsilon z}^2 E_z}{E_z D_z v_{dz}^2} \end{matrix} \right\} = \left\{ \begin{matrix} \frac{v_{\epsilon x}^2}{v_{dx}^2} \\ \frac{v_{\epsilon y}^2}{v_{dy}^2} \\ \frac{v_{\epsilon z}^2}{v_{dz}^2} \end{matrix} \right\} \quad (2.5.12)$$

Also note that the dielectric (ϵ) and permeability (k_m) are

related as follows:

$$k_m = \epsilon \left(\frac{m_t}{m_e} \right)^{\frac{3}{2}} \cos^2(\theta) \quad (2.5.12a)$$

Then the De Broglie velocities are defined in terms of the speed of light then v_{dx} , v_{dy} and v_{dz} as per equations 2.4.1, 2.4.2, 2.4.3 can be considered a modified speeds of light internal to the superconductor material as per equation 2.5.13. These relativistic De Broglie velocities are presented in equation 2.5.12 with results also presented in terms of wave vectors K_A , K_B and K_P .

$$\left. \begin{matrix} v_{dx} \\ v_{dy} \\ v_{dz} \end{matrix} \right\} = \left\{ \begin{matrix} \frac{c}{\sqrt{k_m \epsilon_x}} \\ \frac{c}{\sqrt{k_m \epsilon_y}} \\ \frac{c}{\sqrt{k_m \epsilon_z}} \end{matrix} \right\} = \left\{ \begin{matrix} \frac{c}{\sqrt{k_m \frac{D_x}{E_x}}} \\ \frac{c}{\sqrt{k_m \frac{D_y}{E_y}}} \\ \frac{c}{\sqrt{k_m \frac{D_z}{E_z}}} \end{matrix} \right\} \quad (2.5.13a)$$

and

$$\left. \begin{matrix} v_{dx} \\ v_{dy} \\ v_{dz} \end{matrix} \right\} = \left\{ \begin{matrix} \frac{c}{\sqrt{k_m 8 \frac{B}{A} \frac{\mathbb{C}^2 e_{\pm}^2 m_t}{\sqrt{3} \hbar^2 K_B}}} \\ \frac{c}{\sqrt{k_m 4 \frac{B}{A} \frac{\mathbb{C}^2 e_{\pm}^2 m_t}{\hbar^2 K_P}}} \\ \frac{c}{\sqrt{k_m 4 \frac{\mathbb{C}^2 e_{\pm}^2 m_t}{\sqrt{3} \hbar^2 K_A}}} \end{matrix} \right\} = \left\{ \begin{matrix} \frac{v_{\epsilon x}^2}{3^{1/4} \frac{B}{A} c} \\ \frac{K_B}{K_P} \frac{v_{\epsilon y}^2}{3^{1/4} \frac{B}{A} c} \\ \frac{K_B}{K_A} \frac{v_{\epsilon z}^2}{3^{1/4} \frac{B}{A} c} \end{matrix} \right\} \quad (2.5.13b)$$

Combining equations 2.5.12 and 2.5.13, the Cartesian dielectric velocities can be computed and are presented in Table 2.5.2.

Table 2.5.2

$T_c (^{\circ}K)$	3,100,000	2,135	1,190	447	93	8.11E-15
$T_b (^{\circ}K)$	1.3E+11	3.4E+09	2.5E+09	1.6E+09	7.1E+08	2.729
k_m	1.0E+03	3.9E+04	5.2E+04	8.4E+04	1.9E+05	6.3E+13
v_{ex} (cm/sec)	2.9E+09	4.8E+08	4.1E+08	3.2E+08	2.2E+08	1.2E+04
v_{ey} (cm/sec)	3.4E+09	5.5E+08	4.8E+08	3.7E+08	2.5E+08	1.4E+04
v_{ez} (cm/sec)	1.4E+10	2.3E+09	2.0E+09	1.5E+09	1.0E+09	5.6E+04

We note with special interest that the Lorentz-Einstein relativistic relationship expressed in equation 2.5.14 equals 2 which we define as *Cooper* for all T_c .

$$\frac{1}{\sqrt{1 - \frac{v_{dx}^2}{c^2}}} = \mathbb{C} = 2$$

and

$$\left\{ \begin{array}{l} \frac{1}{1 - \sqrt{1 - \frac{v_{ex}^2}{c^2}}} \\ \frac{1}{1 - \sqrt{1 - \frac{v_{ey}^2}{c^2}}} \\ \frac{1}{1 - \sqrt{1 - \frac{v_{ez}^2}{c^2}}} \end{array} \right\} = \left\{ \begin{array}{l} \frac{1}{1 - \sqrt{1 - \sqrt{3} \frac{B^2}{A^2} \frac{v_{dx}^2}{v_{ex}^2}}} \\ \frac{1}{1 - \sqrt{1 - \sqrt{3} \frac{K_P^2 B^2}{K_B^2 A^2} \frac{v_{dx}^2}{v_{ey}^2}}} \\ \frac{1}{1 - \sqrt{1 - \sqrt{3} \frac{K_A^2 B^2}{K_B^2 A^2} \frac{v_{dx}^2}{v_{ez}^2}}} \end{array} \right\} \quad (2.5.14)$$

As a check on these dielectric Cartesian velocities, note that they are vectorially related to v_{ϵ} from equation 2.5.5 as indicated in equation 2.5.14. As indicated, the factor '2' is related to the ratio of Cartesian surfaces *approach*, *section* and *side* to trisine area $\cos(\theta)/\text{section}$ and *cavity/chain*.

$$\begin{aligned} & (\text{approach}) \left(\frac{\cos(\theta)}{\text{section}} \right) \left(\frac{\text{chain}}{\text{cavity}} \right) \\ & + (\text{section}) \left(\frac{\cos(\theta)}{\text{section}} \right) \left(\frac{\text{chain}}{\text{cavity}} \right) \\ & + (\text{side}) \left(\frac{\cos(\theta)}{\text{section}} \right) \left(\frac{\text{chain}}{\text{cavity}} \right) = 2 \end{aligned} \quad (2.5.15)$$

$$v_{\epsilon} = 2\sqrt{v_{\epsilon x}^2 + v_{\epsilon y}^2 + v_{\epsilon z}^2}$$

Based on the Cartesian dielectric velocities, corresponding Cartesian fluxoids can be computed as per equation 2.5.16.

$$\left\{ \begin{array}{l} \Phi_{\epsilon x} \\ \Phi_{\epsilon y} \\ \Phi_{\epsilon z} \end{array} \right\} = \left\{ \begin{array}{l} \frac{2\pi\hbar v_{\epsilon x}}{\text{Cooper } e_{\pm}} \\ \frac{2\pi\hbar v_{\epsilon y}}{\text{Cooper } e_{\pm}} \\ \frac{2\pi\hbar v_{\epsilon z}}{\text{Cooper } e_{\pm}} \end{array} \right\} \quad (2.5.16)$$

The trisine residence *relativistic CPT time*_± is confirmed in terms of conventional capacitance(*C*) and inductance(*L*) resonance circuit relationships in *x*, *y* and *z* as well as *trisine* dimensions.

$$\begin{aligned}
 time_{\pm} &= \left\{ \begin{array}{l} \sqrt{L_x \sqrt{C_x}} \\ \sqrt{L_y \sqrt{C_y}} \\ \sqrt{L_z \sqrt{C_z}} \\ \sqrt{L \sqrt{C}} \end{array} \right\} \quad (2.5.17) \\
 &= \left\{ \begin{array}{l} \sqrt{\frac{\Phi_x \text{ time}}{C e_{\pm} v_{\epsilon x}} \sqrt{\frac{\text{approach } \epsilon_x}{4\pi 2B}}} \\ \sqrt{\frac{\Phi_y \text{ time}}{C e_{\pm} v_{\epsilon y}} \sqrt{\frac{\text{side } \sqrt{3}\epsilon_y}{4\pi 3B}}} \\ \sqrt{\frac{\Phi_z \text{ time}}{C e_{\pm} v_{\epsilon z}} \sqrt{\frac{\text{section } \epsilon_z}{4\pi A}}} \\ \sqrt{\frac{\Phi \text{ time}}{C e_{\pm} v_{\epsilon}} \sqrt{\frac{1}{g_s^2} \frac{\text{section } 2 \text{ section } \epsilon}{4\pi \cos(\theta) \text{ cavity } \cos(\theta)}}} \end{array} \right\}
 \end{aligned}$$

Where relationships between Cartesian and trisine capacitance and inductance is as follows:

$$2 C = C_x = C_y = C_z \quad (2.5.18)$$

$$L = 2 L_x = 2 L_y = 2 L_z \quad (2.5.19)$$

$$L_x = L_y = L_z \quad (2.5.20)$$

$$C_x = C_y = C_z \quad (2.5.21)$$

Table 2.5.3

$T_i (^{\circ}K)$	3,100,000	2,135	1,190	447	93	8.1E-16
$T_s (^{\circ}K)$	1.3E+11	3.4E+09	2.5E+09	1.6E+09	7.1E+08	2.729
C/v (fd/cm ³)	1.4E+06	3.8E+04	2.8E+04	1.7E+04	7.9E+03	2.3E-05
L/v (h/cm ³)	9.0E+15	2.4E+14	1.8E+14	1.1E+14	4.9E+13	1.5E+05

In terms of an extended Thompson cross section(σ_T), it is noted that the $(1/R^2)$ factor [62] is analogous to a dielectric(ϵ) equation 2.5.4. Dimensionally the dielectric (ϵ) is proportional to trisine cell length dimension.

The extended Thompson scattering cross section (σ_T) [43 equation 78.5, 62 equation 33] then becomes as in equation 2.5.22.

$$\sigma_T = \left(\frac{K_B}{K_{Ds}} \right)^2 \left(\frac{8\pi}{3} \right) \left(\frac{e_{\pm}^2}{\epsilon m_t v_{dy}^2} \right)^2 \approx \text{side} \quad (2.5.22)$$

2.6 FLUXOID AND CRITICAL FIELDS

Based on the material fluxoid(Φ_{ϵ}) (equation 2.5.5), the critical fields (H_{c1}) (equation 2.6.1), (H_{c2}) (equation 2.6.2) & (H_c) (equation 2.6.3) as well as penetration depth(λ) (equation 2.6.5) and Ginzburg-Landau coherence length (ξ) (equation 2.6.6) are computed. Also the critical field (H_c) is alternately computed from a variation on the Biot-Savart law.

$$H_{c1} = \frac{\Phi_{\epsilon}}{\pi \lambda_t^2} \quad (2.6.1)$$

$$\begin{aligned}
 H_{c2} &= \frac{4\pi C}{\text{section}} \Phi_{\epsilon} \quad (2.6.2) \\
 &= \left(\frac{1}{g_s} \right) \frac{4\pi}{\pi \left(\frac{B}{\sqrt{2}} \right)^2} \Phi_{\epsilon} \cos(\theta)
 \end{aligned}$$

$$H_c = \sqrt{H_{c1} H_{c2}} = \frac{e_{\pm}}{v_{\epsilon x} \cdot A \cdot \text{time}} \frac{m_t}{m_e} \quad (2.6.3)$$

$$n_c = \frac{C}{\text{cavity}} \quad (2.6.4)$$

Also it interesting to note that the following relationship holds

$$2\pi \frac{e_{\pm}^2}{A B} = m_e v_{dx}^2 m_e c^2 \quad (2.6.4a)$$

Figure 2.6.1 Experimental (Harshman Data) and Trisine Model Cooper CPT Charge conjugated Pair Three Dimensional Concentration as per equation 2.6.4

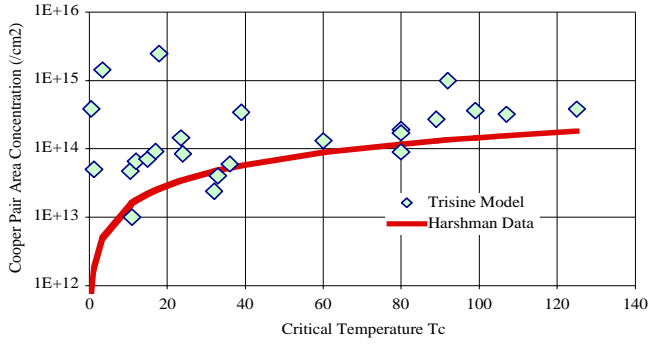
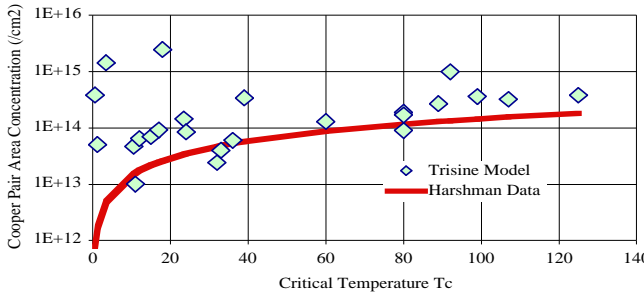


Figure 2.6.2 Experimental (Harshman Data) and Trisine Model Cooper CPT Charge conjugated Pair Two Dimensional Area Concentration or \mathbb{C} /section



$$\lambda^2 = \left(\frac{1}{g_s^2} \right) \mathbb{C} \left(\frac{m_t v_\varepsilon^2}{2} \right) \frac{1}{n_c} \frac{1}{(\mathbb{C} e)^2} \quad (2.6.5)$$

$$= \left(\frac{1}{g_s^2} \right) \mathbb{C} \left(\frac{1}{\varepsilon} \right) \left(\frac{m_t c^2}{2} \right) \frac{1}{n_c} \frac{1}{(\mathbb{C} e_\pm)^2}$$

From equation 2.6.5, the trisine penetration depth λ is calculated. This is plotted in the above figure along with Harshman[17] and Homes[51, 59] penetration data. The Homes data is multiplied by a factor of $(n_e \text{ chain}/\text{Cooper})^{1/2}$ to get n_c in equation 2.6.5. This is consistent with $\lambda^2 \propto 1/n_c$ in equation 2.6.5. It appears to be a good fit and better than the fit with data compiled by Harshman[17].

Penetration depth and gap data for magnesium diboride MgB_2 [55] which has a critical temperature T_c of 39 K indicates a fit to the trisine model when a critical temperature of 39/3 or 13

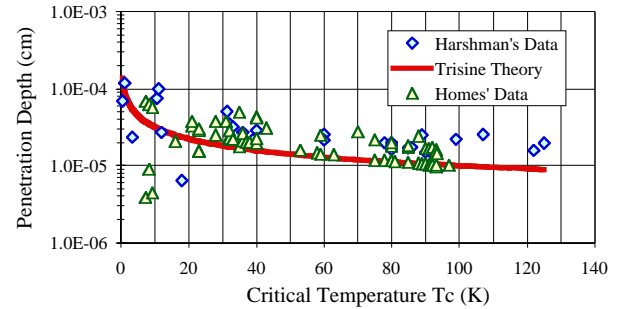
K is assumed (see Table 2.6.1). This is interpreted as an indication that MgB_2 is a three dimensional superconductor.

Table 2.6.1 Experimental (MgB_2 Data[55]) and Trisine Model Prediction

	Trisine Data at T_c 39/3 K or 13 K	Observed Data [55]
Penetration Depth (nm)	276	260 \pm 20
Gap (meV)	1.12	3.3/3 or 1.1 \pm .3

As indicated in equation 2.5.5, the material dielectric modified speed of light v_ε is a function of material dielectric (ε) constant which is calculated in general and specifically for trisine by $\varepsilon = D/E$ (equation 2.5.4). The fact that chain rather than cavity (related by 2/3 factor) must be used in obtaining a trisine model fit to Homes' data indicates that the stripe concept may be valid in as much as chains in the trisine lattice visually form a striped pattern as in Figure 2.3.1.

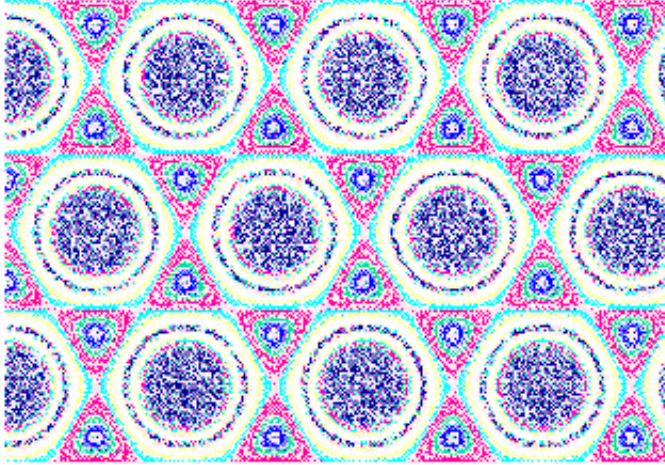
Figure 2.6.3 Experimental (Homer and Harshmann) and Trisine Model Penetration Depth



See derivation of Ginzberg-Landau coherence length ξ in equation 2.6.6 in Appendix D. It is interesting to note that $tB/\xi = 2.73 \approx e$ for all T_c which makes the trisine superconductor mode fit the conventional description of operating in the "dirty" limit. [54]

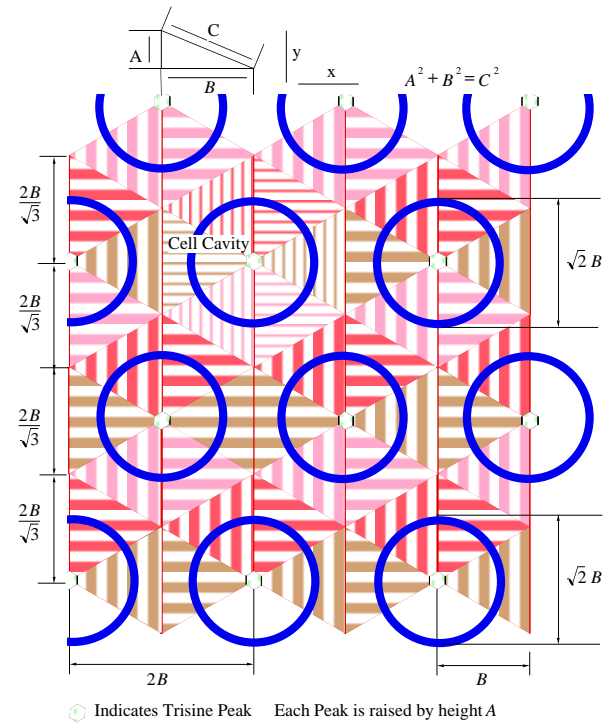
$$\xi = \sqrt{\frac{m_t}{m_e} \frac{1}{K_B^2} \frac{\text{chain}}{\text{cavity}}} \quad (2.6.6)$$

Figure 2.6.4 Trisine Geometry in the Fluxoid Mode (Interference Pattern Ψ^2)



The geometry presented in Figure 2.6.4 is produced by three intersecting coherent polarized standing waves which can be called the trisine wave function. It is interesting to note that a singularity exists at the circular portion. This is similar to the singularity at the Schwarzschild radius as derived in the general theory of relativity. This can be compared to figure 2.6.5 which presents the dimensional trisine geometry.

Figure 2.6.5 Trisine Geometry in the Fluxoid Mode



Equation 2.6.7 represents the trisine wave function (Ψ). This wave function is the addition of three sin functions that are 120 degrees from each other in the x y plane and form an angle 22.8 degrees with this same x y plane. Also note that 22.8 degrees is related to the (B/A) ratio by $\tan(90^\circ - 22.8^\circ) = B/A$.

$$\Psi = e^{\sin\left(2\left(a_{x1}x_0+b_{x1}y_0+c_{x1}z_0\right)\right)} + e^{\sin\left(2\left(a_{x2}x_0+b_{x2}y_0+c_{x2}z_0\right)\right)} + e^{\sin\left(2\left(a_{x3}x_0+b_{x3}y_0+c_{x3}z_0\right)\right)} \quad (2.6.7)$$

Where:

$$a_{x1} = \cos(030^\circ)\cos(22.8^\circ)$$

$$b_{x1} = \sin(030^\circ)\cos(22.8^\circ)$$

$$c_{x1} = -\sin(030^\circ)$$

$$a_{x2} = \cos(150^\circ)\cos(22.8^\circ)$$

$$b_{x2} = \sin(150^\circ)\cos(22.8^\circ)$$

$$c_{x2} = -\sin(150^\circ)$$

$$a_{x3} = \cos(270^\circ)\cos(22.8^\circ)$$

$$b_{x3} = \sin(270^\circ)\cos(22.8^\circ)$$

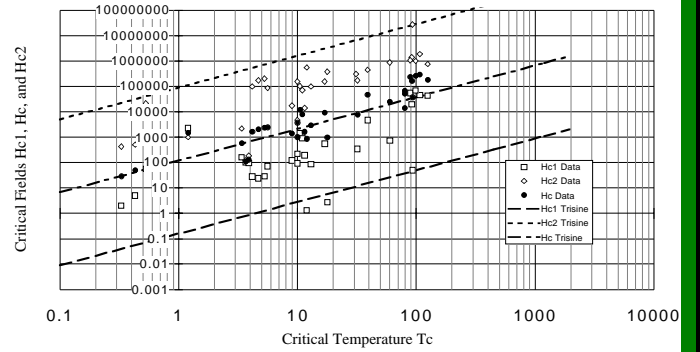
$$c_{x3} = -\sin(270^\circ)$$

In table 2.6.2, note that the ratio of London penetration length(λ) to Ginzburg-Landau correlation distance(ξ) is the constant(κ) of 58. The trisine values compares favorably with London penetration length(λ) and constant(κ) of 1155(3) Å and 68 respectively as reported in reference [11, 17] based on experimental data.

Table 2.6.2

T_c ($^\circ K$)	3,100,000	2,135	1,190	447	93	8.1E-16
T_c ($^\circ K$)	1.3E+11	3.4E+09	2.5E+09	1.6E+09	7.1E+08	2.729
H_c (gauss)	1.6E+10	1.7E+06	8.4E+05	2.5E+05	3.5E+04	1.6E-17
H_{c1} (gauss)	2.1E+07	2.3E+03	1.1E+03	3.3E+02	4.6E+01	2.2E-20
H_{c2} (gauss)	1.2E+13	1.3E+09	6.3E+08	1.9E+08	2.6E+07	1.2E-14
n_c (/cm ³)	3.0E+28	5.4E+23	2.3E+23	5.2E+22	4.9E+21	1.3E-04
λ (cm)	5.7E-08	2.2E-06	2.9E-06	4.7E-06	1.0E-05	3500
ξ (cm)	9.8E-10	3.7E-08	5.0E-08	8.1E-08	1.8E-07	60.30

Figure 2.6.5 Critical Magnetic Field Data (gauss) compared to Trisine Model as a function of T_c



2.7 SUPERCONDUCTOR INTERNAL PRESSURE

The following pressure values in Table 2.7.1 as based on equations 2.7.1 indicate rather high values as superconducting (T_c) increases. This is an indication of the rather large forces that must be contained in these anticipated materials.

$$pressure = \left\{ \begin{array}{l} \frac{\hbar K_B}{time_{\pm} \text{ approach}} \\ \frac{\hbar K_P}{time_{\pm} \text{ side}} \\ \frac{\hbar K_A}{time_{\pm} \text{ section}} \end{array} \right\} = \left\{ \begin{array}{l} \frac{F_x}{\text{approach}} \\ \frac{F_y}{\text{side}} \\ \frac{F_z}{\text{section}} \end{array} \right\} \quad (2.7.1a)$$

$$\begin{aligned}
 \text{pressure} &= \left\{ \begin{array}{l} \frac{m_t v_{dx}}{\text{time approach}} \\ \frac{m_t v_{dy}}{\text{time side}} \\ \frac{m_t v_{dz}}{\text{time section}} \end{array} \right\} \\
 &= \frac{\text{Cooper } k_b T_c}{\text{cavity}} \\
 &= \frac{\sqrt{A^2 + B^2}}{B} \frac{\text{cavity } \pi^2 \hbar v_{dx}}{\text{chain } 240 A^4} \\
 &\quad \text{(Casimir pressure)}
 \end{aligned} \tag{2.7.1b}$$

To put the calculated pressures in perspective, the C-C bond has a reported energy of 88 kcal/mole and a bond length of 1.54 Å [24]. Given these parameters, the internal chemical bond pressure (CBP) for this bond is estimated to be:

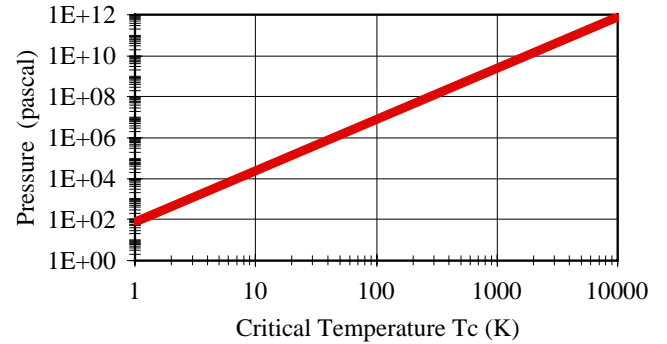
$$\begin{aligned}
 \text{CBP} &= 88 \frac{\text{kcal}}{\text{mole}} \cdot 4.18 \times 10^{10} \frac{\text{erg}}{\text{kcal}} \\
 &\quad \cdot \frac{1}{6.02 \times 10^{23}} \frac{\text{mole}}{\text{bond}} \\
 &\quad \cdot \frac{1}{(1.54 \times 10^{-8})^3} \frac{\text{bond}}{\text{cm}^3} \\
 &= 1.67 \times 10^{12} \frac{\text{erg}}{\text{cm}^3}
 \end{aligned}$$

Within the context of the superconductor internal pressure numbers in table 2.7.1, the internal pressure requirement for the superconductor is less than the C-C chemical bond pressure at the order of design T_c of a few thousand degrees Kelvin indicating that there is the possibility of using materials with the bond strength of carbon to chemically engineer high performance superconducting materials.

In the context of interstellar space vacuum, the total pressure $m_t c^2 / \text{cavity}$ may be available and will be of such a magnitude as to provide for universe expansion as astronomically observed. (see equation 2.11.21)

Table 2.7.1 with pressure plot

T_c ($^{\circ}K$)	3,100,000	2,135	1,190	447	93	8.1E-16
T_c ($^{\circ}K$)	1.3E+11	3.4E+09	2.5E+09	1.6E+09	7.1E+08	2.729
pressure erg/cm ³	1.3E+19	1.6E+11	3.7E+10	3.2E+09	6.3E+07	1.4E-35
pressure (psi)	1.9E+14	2.3E+06	5.4E+05	4.7E+04	9.2E+02	2.1E-40
pressure (pascal)	1.3E+18	1.6E+10	3.7E+09	3.2E+08	6.3E+06	1.4E-36
Total pressure erg/cm ³	1.36E+24	2.45E+19	1.02E+19	2.35E+18	2.23E+17	5.73E-09



Assuming the superconducting current moves as a longitudinal wave with an adiabatic character, then equation 2.7.2 for current or De Broglie velocity (v_{dx}) holds where the ratio of heat capacity at constant pressure to the heat capacity at constant volume (δ) equals 1.

$$v_{dx} = \sqrt{\delta \text{ pressure} \frac{\text{cavity}}{m_t}} \tag{2.7.2}$$

The Casimir force is related to the trisine geometry by equation 2.7.3.

$$\text{Casimir Force} = g_s^3 \frac{\text{section}}{3} \frac{\pi^2 \hbar v_{dz}}{240 A^4} \tag{2.7.3}$$

In a recent report[53] by Jet Propulsion Laboratory, an unmodeled deceleration was observed in regards to Pioneer 10 and 11 spacecraft as they exited the solar system. This drag can be related to the following expression where (m_t / cavity) is the mass equivalent energy density value at $T_c = 8.1 \times 10^{-16} \text{ } ^{\circ}K$ representing conditions in space which is 100 percent transferred to an object passing through it.

$$\text{Drag Force} = -\text{AREA} \frac{m_t}{\text{cavity}} c^2 \tag{2.7.4}$$

Note that equation 2.7.4 is similar to the conventional drag equation as used in design of aircraft with v^2 replaced with c^2 . Of course $Drag\ Force = Ma$, so the Pioneer space craft $M / AREA$, is an important factor in establishing deceleration which was observed to be on the order of $8.74E-8\ cm^2/sec$.

The drag equation is repeated below in terms of Pioneer spacecraft and the assumption that space density is essentially what has been empirically determined to be dark matter:

$$F = Ma = C_d A_c \rho \frac{v^2}{2} \quad (2.7.4)$$

where :

$$C_d = \frac{24}{R_e} + \frac{6}{1 + \sqrt{R_e}} + .4 \quad [60] \text{ empirical}$$

where :

F = force

M = Pioneer 10 & 11 Mass

a = acceleration

A_c = Pioneer 10 & 11 cross section

ρ = space fluid density ($6.38 \times 10^{-30}\ g/cm^3$)
consistent with dark matter estimates

v = object velocity

μ = absolute fluid viscosity ($1.21E-16\ g/(cm\ sec)$)

ν = kinematic fluid viscosity μ / ρ ($1.90 \times 10^{13}\ cm^2/sec$)

R_e = Reynolds' number

$$= \frac{\text{inertial force}}{\text{viscous force}} = \text{dimensionless number}$$

$$= \frac{\rho v D}{\mu} = \frac{(\text{fluid density})(\text{object velocity})(\text{object diameter})}{(\text{fluid absolute viscosity})}$$

When the Reynolds' number is low (laminar flow condition), then $C_d = (24/R_e)$ and the drag equation reduces to the Stokes' equation $F = 3\pi\mu\nu D$. [60]

In other parts of this report, a model is developed as to what this dark matter actually is. The model dark matter is keyed to a $6.38E-30\ g/cc$ value in trisine model (NASA observed value of $6E-30\ g/cc$). The proposed dark matter consists of mass units of m_t ($110 \times$ electron mass) per volume (cavity- $15733\ cm^3$). These mass units are virtual particles that exist in a coordinated lattice at base energy $\hbar\omega/2$ under the condition that momentum and energy are conserved - in other words complete elasticity. This dark matter lattice would have internal pressure (table 2.7.1) to withstand collapse into gravitational clumps.

Under these circumstances, the traditional drag equation form is valid but velocity (v) should be replaced by speed of light (c). Correspondingly, the space viscosity is computed as momentum/area or $(m_t c / (2\Delta x^2))$ where Δx is uncertainty dimension in table 2.5.1 at $T_c = 8.1E-16\ K$ and as per equation 2.1.20. This is in general agreement with gaseous kinetic theory [19].

$$\int_0^B F dx = m_t \int_0^{v_{dx}} \frac{v}{\sqrt{1 - \frac{v^2}{c^2}}} dv \quad (2.7.5)$$

$$\text{where } m_t = \frac{\hbar K_B}{v_{dx}} = \frac{\hbar}{v_{dx}} \frac{\pi}{B} = \frac{\hbar}{2 \Delta v \Delta x}$$

$$\text{and } m_t = \frac{\Delta v}{v_{dx}} = \frac{1}{2\pi} \frac{B}{\Delta x}$$

$$\text{and } \Delta v = 0 \rightarrow v_{dx} \text{ and } \Delta x = 0 \rightarrow B$$

then

$$F B = -m_t c^2 \sqrt{1 - \frac{v_{dx}^2}{c^2}} \\ = -m_t c^2 \text{ at } v_{dx} \ll c$$

It is understood that the above development assumes that $dv/dt \neq 0$, an approach which is not covered in standard texts[61], but is assumed to be valid here because of dimensional similarity to the Heisenberg Uncertainty principle as reflected in equation 2.1.20 and also applicability in a collision context.

In terms of an object passing through the trisine elastic space CPT lattice at some velocity $v = v_{dx} x/B$, the force (F) is no longer dependent of object velocity (v) at $v_{dx} < v \ll c$ but is a constant relative to c^2 which reflects the fact that the speed of light is a constant in the universe and in consideration of the following established relationship:

$$F = -C_d \frac{m_t c^2}{x} \quad (2.7.6)$$

Where C_d is the standard fluid mechanical drag coefficient.

This model was used to analyze the Pioneer Unmodeled Deceleration data $8.74E-08\ cm/sec^2$ and there appeared to be a good fit with the observed space density $6E-30\ g/cm^3$ (trisine model $6.38E-30\ g/cm^3$). A drag coefficient of 59.67 indicates a laminar flow condition. An absolute space viscosity of $1.21E-16\ g/(cm\ sec)$ is established within trisine model and used.

Pioneer (P) Translational Calculations

P mass	241,000 gram
P diameter	274 cm (effective)
P cross section	58,965 cm^2 (effective)

P area/mass	0.24	cm ² /g
P velocity	1,117,600	cm/sec
space kinematic viscosity	1.90E+13	cm ² /sec
space density	6.38E-30	g/cm ³
Pioneer Reynold's number	4.31E-01	unitless
drag coefficient	59.67	
P deceleration	8.37E-08	cm/sec ²
one year drag distance	258.51	mile
laminar drag force	9.40E-03	dyne
Time of object to stop	1.34E+13	sec

JPL, NASA raised a question concerning the universal application of the observed deceleration on Pioneer 10 & 11. In other words, why do not the planets and their satellites experience such an deceleration? The answer is in the A_c/M ratio in the modified drag relationship.

$$a = -C_d \frac{m_t c^2}{x} = -C_d \frac{A_c}{M} \rho c^2 = -C_d \frac{A_c}{M} \frac{m_t}{cavity} c^2 \quad (2.7.6)$$

Using the earth as an example, the earth differential movement per year due to modeled deceleration of $4.94E-19$ cm/sec² would be 0.000246 centimeters (calculated as $at^2/2$, an unobservable distance amount). Also assuming the trisine superconductor model, the reported 6 nanoTesla (nT) (6E-5 gauss) interplanetary magnetic field (IMF) in the vicinity of earth, will not allow the formation of a superconductor CPT lattice due to the well known properties of a superconductor in that magnetic fields above critical fields will destroy it. In this case, the space superconductor at $T_c = 8.1E-16$ K will be destroyed by a critical magnetic field above $H_{c2} = 2.14E-14$ gauss as in table 2.6.1. It is conceivable that the IMF decreases by some power law with distance from the sun, and perhaps at some distance the IMF diminishes to an extent wherein the space superconductor CPT lattice is allowed to form. This may be an explanation for the observed "kick in" of the Pioneer spacecraft deceleration phenomenon at 10 Astronomical Units (AU).

Earth Translational Calculations

Earth mass	5.98E+27	gram
Earth diameter	1.27E+09	cm
Earth cross section	1.28E+18	cm ²
Earth area/mass	2.13E-10	cm ² /g
Earth velocity	2,980,010	cm/sec
space kinematic viscosity	1.90E+13	cm ² /sec
space density	6.38E-30	g/cm ³
Earth Reynold's number	2.01E+06	unitless
drag coefficient	0.40	unitless
drag force (with drag coefficient)	2.954E+09	dyne
Earth deceleration	4.94E-19	cm/sec ²
One year drag distance	0.000246	cm

laminar drag force	4.61E-01	dyne
Time for Earth to stop rotating	6.03E+24	sec

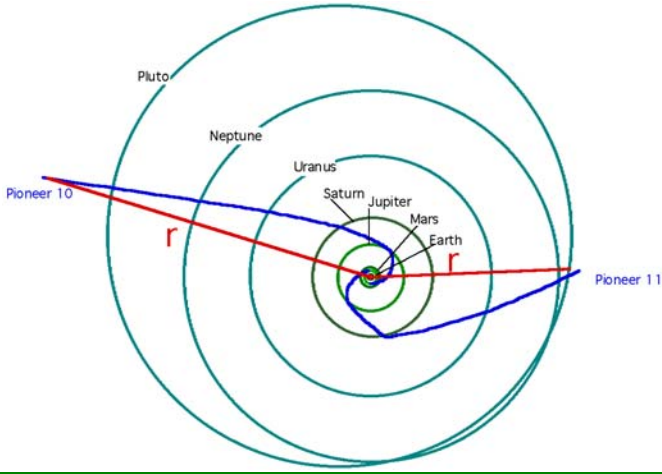
Now to test the universal applicability of the unmodeled Pioneer 10 & 11 decelerations for other man made satellites, one can use the dimensions and mass of the Hubble space telescope. One arrives at a smaller deceleration of $6.79E-09$ cm/sec² because of its smaller area/mass ratio. This low deceleration is swamped by other decelerations in the vicinity of earth, which would be multiples of those well detailed in reference 1, Table II Pioneer Deceleration Budget. Also the trisine elastic space CPT lattice probably does not exist in the immediate vicinity of the earth because of the earth's milligauss magnetic field which would destroy the coherence of the trisine elastic space CPT lattice.

Hubble Satellite Translational Calculations

Hubble mass	1.11E+07	gram
Hubble diameter	7.45E+02	centimeter
Hubble cross section	5.54E+05	cm ²
Hubble area/mass	0.0499	cm ² /g
Hubble velocity	790,183	cm/sec
space kinematic viscosity	1.90E+13	cm ² /sec
space density	6.38E-30	g/cm ³
Hubble Reynolds' number	1.17E+00	unitless
drag coefficient	23.76	
drag force (with drag coefficient)	7.549E-02	dyne
Hubble deceleration	6.79E-09	cm/sec ²
One year drag distance	3,378,634	cm
laminar drag force	7.15E-08	dyne
Time for Hubble to stop rotating	1.16E+14	sec

The fact that the unmodeled Pioneer 10 & 11 deceleration data are statistically equal to each other and the two space craft exited the solar system essentially 190 degrees from each other implies that the supporting fluid space density through which they are traveling is co-moving with the solar system. But this may not be the case. Assuming that the supporting fluid density is actually related to the cosmic background microwave radiation (CMBR), it is known that the solar system is moving at 500 km/sec relative to CMBR. Equivalent decelerations in irrespective to spacecraft heading relative to the CMBR would further support the hypothesis that deceleration is independent of spacecraft velocity.

Figure 2.7.1 Pioneer Trajectories (NASA JPL [53]) with delineated solar satellite radial component r .



Executing a web based [58] computerized radial rate dr/dt (where r is distance of spacecraft to sun) of Pioneer 10 & 11 (Figure 2.7.1), it is apparent that the solar systems exiting velocities are not equal. Based on this graphical method, the spacecraft's velocities were in a range of about 9% (28,600 – 27,500 mph for Pioneer 10 “3Jan87 - 22July88” and 26,145 – 26,339 mph for Pioneer 11 ”5Jan87 - 01Oct90”). This reaffirms the basic drag equation used for computation in that, velocity magnitude of the spacecraft is not a factor, only its direction with the drag force opposite to that direction. The observed equal deceleration at different velocities would appear to rule out deceleration due to Kuiper belt dust as a source of the deceleration for a variation at 1.09^2 or 1.19 would be expected.

Also it is observed that the Pioneer spacecraft spin is slowing down from 7.32 rpm in 1987 to 7.23 rpm in 1991. This equates to an angular deceleration of .0225 rpm/year or $1.19E-11$ rotation/sec². JPL[57] has acknowledged some systematic forces that may contribute to this deceleration rate and suggests an unmodeled deceleration rate of .0067 rpm/year or $3.54E-12$ rotations/sec. [57]

Now using the standard torque formula:

$$\Gamma = I\dot{\omega} \quad (2.7.7)$$

The deceleration value of $3.54E-12$ rotation/sec² can be replicated assuming a Pioneer Moment of Inertia about spin axis(I) of $5.88E+09$ g cm² and a 'paddle' cross section area of $3,874$ cm² which is 6.5 % spacecraft 'frontal' cross section which seems reasonable. The gross spin deceleration rate of .0225 rpm/year or $1.19E-11$ rotation/sec² results in a pseudo

paddle area of $13,000$ cm² or 22.1% of spacecraft 'frontal' cross section which again seems reasonable.

Also it is important to note that the angular deceleration rate for each spacecraft (Pioneer 10, 11) is the same even though they are spinning at the two angular rates 4 and 7 rpm respectfully. This would further confirm that velocity is not a factor in measuring the space mass or energy density. The calculations below are based on NASA JPL problem set values[57]. Also, the sun is moving through the CMBR at 600 km/sec. According to this theory, this velocity would not be a factor in the spacecraft deceleration.

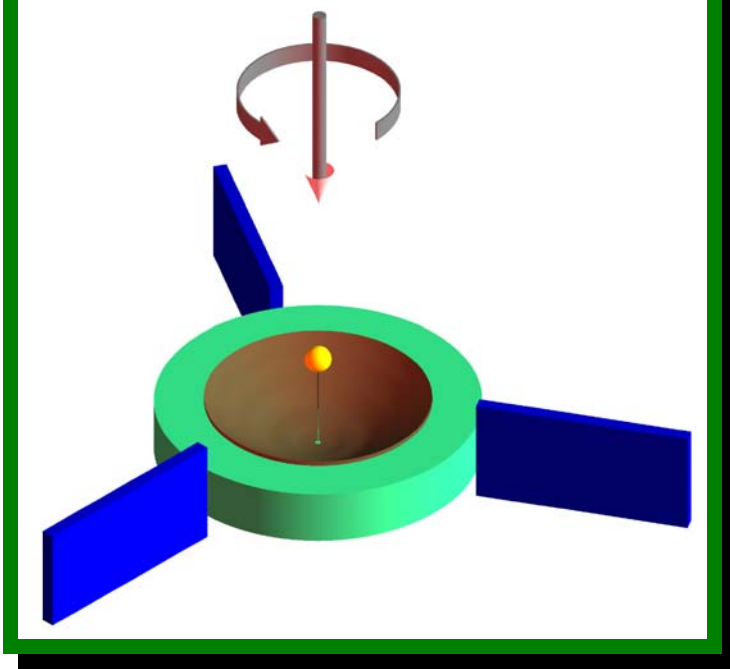
Pioneer (P) Rotational Calculations

P mass	241,000	g
P moment of inertia	$5.88E+09$	g cm ²
P diameter	274	cm
P translational cross section	58,965	cm ²
P radius of gyration k	99	cm
P radius r	137	cm
paddle cross section	3,874	cm ²
paddle area/mass	0.02	cm ² /g
P rotation speed at k	4,517	cm/sec
P rotation rate change	0.0067	rpm/year
P rotation rate change	$3.54E-12$	rotation/sec ²
P rotation rate change	$2.22E-11$	radian/sec ²
P rotation deceleration at k	$2.20E-09$	cm/sec ²
P force slowing it down	$1.32E-03$	dyne
space kinematic viscosity	$1.90E+13$	cm ² /sec
space density	$6.38E-30$	g/cm ³
P Reynolds' number	$4.31E-01$	unitless
drag coefficient	59.67	
drag force	$1.32E-03$	dyne
P Paddle rotational deceleration at k	$2.23E-11$	radian/sec ²
P Paddle rotational deceleration at k	$2.20E-09$	cm/sec ²
One year rotational drag distance	1,093,344	cm
P rotational laminar drag force	$7.32E-23$	dyne
Time for P to stop rotating	$2.05E+12$	sec

These calculations suggest a future spacecraft with general design below to test this hypothesis. This design incorporates general features to measure translational and rotational drag. A wide spectrum of variations on this theme are envisioned. General Space Craft dimensions should be on the order of Trisine geometry B at $T_b = 2.711 K$ $T_c = 8.12E-16 K$ or 22 cm (Table 2.2.1) or larger. The Space Craft Reynold's number would be nearly 1 at this dimension and the resulting drag the greatest. The coefficient of drag would decrease towards one with larger Space Craft dimensions. It is difficult to foresee what will happen with Space Craft dimensions

below 22 cm.

Figure 2.7.2 Space craft general design to quantify translational and rotary drag effect. Brown is parabolic antenna, green is translational capture element and blue is rotational capture element.



The spacecraft (Figure 2.7.2) would rotate on green bar axis while traveling in the direction of the green bar. The red paddles would interact with the space matter as mc^2 slowing the rotation with time in conjunction with the overall spacecraft slowing decelerating.

A basic experiment cries out here to be executed and that is to launch a series of spacecraft of varying A_c/M ratios and exiting the solar system at various angles while measuring their rotational and translational decelerations. This would give a more precise measure of the spatial orientation of dark matter in the immediate vicinity of our solar system. An equal calculation of space energy density by translational and rotational observation would add credibility to accumulated data.

The assumption that the Pioneer spacecraft will continue on forever and eventually reach the next star constellation may be wrong. Calculations indicate the Pioneers will come to a stop relative to space fluid in about 400,000 years. We may be more isolated in our celestial position than previously thought.

When this drag model is applied to a generalized design for a Solar Sail [63], a deceleration of $3.49E-05$ cm/sec² is calculated which is 3 orders higher than experienced by Pioneer spacecraft. Consideration should be given to spin paddles for these solar sails in order to accumulate spin

deceleration data also. In general, a solar sail with its characteristic high A_c/M ratio such as this example should be very sensitive to the trisine elastic space CPT lattice. The integrity of the sail should be maintained beyond its projected solar wind usefulness as the space craft travels into space beyond Jupiter.

Pioneer (P) Rotational Calculations

Sail mass	300,000	gram
Sail diameter	40,000	centimeter
Sail cross section	1,256,637,000	cm ²
Sail area/mass	4,189	cm ² /g
Sail velocity	1,117,600	cm/sec
space kinematic viscosity	1.90E+13	cm ² /sec
space density	6.38E-30	g/cm ³
Sail Reynold's number	6.30E+01	unitless
drag coefficient	1.45	
drag force	10	dyne
Sail acceleration	3.49E-05	cm/sec ²
one year drag distance	1.73E+10	cm
laminar drag force	1.37E+00	dyne
Time of Sail to stop	1015	year

The following calculation establishes a distance from the sun at which the elastic space CPT lattice kicks in. There is a energy density competition between the solar wind and the elastic space CPT lattice. Assuming the charged particle density at earth is $5 / \text{cm}^3$ [57] and varying as $1/R^2$ and comparing with elastic space density of kTc/cavity , then an equivalent energy density is achieved at 3.64 AU. This of course is a dynamic situation with solar wind changing with time which would result in the boundary of the elastic space CPT lattice changing with time. This is monitored by a space craft (Advanced Composition Explorer (ACE)) at the L1 position (1% distance to sun) and can be viewed at <http://space.rice.edu/ISTP/dials.html>. A more descriptive term would be making the elastic space CPT lattice decoherent or coherent. It is interesting to note that the calculated boundary is close to that occupied by the Astroids and is considered the Astroid Belt.

Elastic Space CPT lattice intersecting with solar wind

	AU
Mercury	0.39
Venus	0.72
Earth	1.00
Mars	1.53

Jupiter	5.22	
Saturn	9.57	
Uranus	19.26	
Neptune	30.17	
Pluto	39.60	
AU	3.64	
n at AU	0.38	cm ⁻³
r 1/n ^{1/3}	1.38	cm
coordination #	6	unitless
volume	0.44	cm ³
$\frac{e^2}{r} \frac{1}{\text{volume}} \frac{T_c}{T_b}$	$\frac{\text{energy}}{\text{volume}}$	1.13E-34 erg / cm ³
Trisine $\frac{k_b T_c}{\text{cavity}}$	$\frac{\text{energy}}{\text{volume}}$	1.13E-34 erg / cm ³

Now assuming the basic conservation of total kinetic and potential energy for an object in circular orbit of the sun with velocity (v_0) and at distance (R_0) equation 2.7.8 provides an indication of the time required to perturb the object out of the circular orbit in the direction of the sun.

$$v_0^2 + \frac{GM_\odot}{R_0} = v^2 + (v_0 - at)^2$$

$$v_0^2 + \frac{GM_\odot}{R_0} = v^2 + \left(v_0 - C_d \frac{\text{Area}}{M} \rho c^2 t \right)^2 \quad (2.7.8)$$

where $v = \delta v_0$

Assuming the sun orbital velocity perturbing factor δ to be .9 and the time (t) at the estimated age of the solar system (5,000,000,000 years), then the smallest size objects that could remain in sun orbit are listed below as a function of distance (AU) from the sun.

	AU	Space object upper size diameter (meter)
Mercury	0.39	9.04
Venus	0.72	10.67
Earth	1.00	11.63
Mars	1.53	13.04
Jupiter	5.22	18.20
Saturn	9.57	21.50
Uranus	19.26	26.10
Neptune	30.17	29.60
Pluto	39.60	31.96
Kuiper Belt	50	35.95
	60	37.57
	70	39.03
Oort Cloud?	80	40.36
	100	41.60

150	46.75
200	50.82
300	57.20
400	62.24

This calculation would indicate that there is not small particle dust remaining in the solar system, which would include the Kuiper Belt and hypothesized Oort Cloud. Also, the calculated small object size would seem to be consistent with Asteroid Belt objects, which exist at the coherence/decoherence boundary for the elastic space CPT lattice.

This analysis has implications for large-scale galactic structures as well. It is conceivable that energy densities vary spatially within a galaxy with generally increased energy density towards the center. This would imply that a generally radial boundary condition would exist within a galaxy and may be responsible for observed anomalous dark matter galactic rotation. Apparent clumping of galactic matter may be due to localities where elastic space CPT lattice does not exist due to decoherent effects of various energy sources existing at that particular locality. Dark energy and Dark matter may be one and the same.

2.8 SUPERCONDUCTING CURRENT, VOLTAGE AND CONDUCTANCE

The superconducting electrical current (I_e) is expressed as in terms of a volume *chain* containing a Cooper CPT Charge conjugated pair moving through the trisine CPT lattice at a De Broglie velocity (v_{dx}).

$$\frac{I_e}{\text{area}} = \frac{\text{Cooper } e_{\pm} v_{dx}}{\text{chain}} \quad (2.8.1)$$

The superconducting mass current (I_m) is expressed as in terms of a trisine relativistic velocity transformed mass (m_t) per *cavity* containing a Cooper CPT Charge conjugated pair and the *cavity* Cooper CPT Charge conjugated pair residence *relativistic CPT time*_±.

$$I_m = \left(\frac{m_t}{\text{cavity}} \right) \left(\frac{1}{\text{time}} \right) \quad (2.8.2)$$

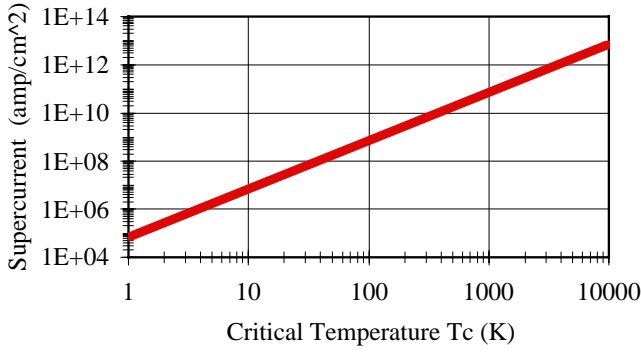
It is recognized that under strict CPT symmetry, there would be zero current flow. It must be assumed that pinning of one side of CPT will result in observed current flow. Pinning

(beyond that which naturally occurs) of course has been observed in real superconductors to enhance actual supercurrents.

Secondarily, this reasoning would provide reasoning why a net charge or current is not observed in a vacuum such as trisine model extended to critical space density in section 2.11.

Table 2.8.1 with super current (amp / cm²) plot.

T_c (°K)	3,100,000	2,135	1,190	447	93	8.1E-16
T_s (°K)	1.3E+11	3.4E+09	2.5E+09	1.6E+09	7.1E+08	2.729
I_c (amp / cm ²)	6.7E+17	3.2E+11	9.8E+10	1.4E+10	6.0E+08	4.6E-26
I_m (g / cm ³ sec)	1.95E+20	2.42E+12	5.62E+11	4.86E+10	9.60E+08	2.2E-34



A standard Ohm's law can be expressed as follows with the resistance expressed as the Hall resistance with a value of 25,815.62 ohms.

$$\text{voltage} = (\text{current}) (\text{resistance})$$

$$\frac{k_b T_c}{\mathbb{C} e_{\pm}} = \left(\frac{\mathbb{C} e_{\pm}}{\text{chain}} \text{ approach } v_{dx} \right) \left(\frac{2\pi\hbar}{(\mathbb{C} e_{\pm})^2} \right) \quad (2.8.3)$$

Equation 2.8.4 represents the Poynting vector relationship or in other words the power per area per relativistic CPT time_± being transmitted from each superconducting cavity:

$$k_b T_c = \frac{m_e}{m_t} \frac{1}{2} E_x H_c (2 \text{ side}) \text{ time}_{\pm} v_{\epsilon} \quad (2.8.4)$$

Equation 2.8.4 can be rearranged in terms of a relationship between the De Broglie velocity (v_{dx}) and modified speed of light velocity ($v_{\epsilon x}$) as expressed in equation 2.8.5.

$$v_{\epsilon x}^2 = \frac{\sqrt{3}}{48\pi^2} \left(\frac{m_t}{m_e} \right)^2 \frac{(\mathbb{C} e_{\pm})^2 B}{\hbar} \frac{B}{A} v_{dx}$$

$$= 3^4 \frac{B}{A} \cdot c \cdot v_{dx} \quad (2.8.5)$$

$$= \pi \cdot c \cdot v_{dx}$$

This leads to the group/phase velocity relationship in equation 2.8.6

$$(\text{group velocity}) \cdot (\text{phase velocity}) = c^2$$

or

$$(2.8.6)$$

$$(v_{dx}) \cdot \left(\frac{1}{\pi} \frac{v_{\epsilon x}^2}{v_{dx}^2} \cdot c \right) = c^2$$

In the Nature reference [51] and in [59], Homes' reports experimental data conforming to the empirical relationship Homes' Law relating superconducting density ρ_s at just above T_c , superconductor conductivity σ_{dc} and T_c .

$$\rho_s \propto \sigma_{dc} T_c \quad \text{Homes' Law ref: 51} \quad (2.8.7)$$

The Trisine model is developed for T_c , but using the Tanner's law observation that $n_s = n_N/4$ (ref 52), we can assume that $E_{fN} = E_{fS}/4$. This is verified by equation 2.5.1. Now substituting E_{fN}/I_c for superconductor conductivity σ_{dc} , and using \mathbb{C}/cavity for super current density ρ_s , the following relationship is obtained and is given the name Homers' constant.

$$\text{Homes' constant} = \frac{\sigma_{dc} k_b T_c}{\rho_s} \quad (2.8.8)$$

$$= \frac{3\pi \mathbb{C}^2 e_{\pm}^2 \hbar A}{2 m_t^2 B}$$

$$= 191,537 \frac{\text{cm}^5}{\text{sec}^3}$$

The results for both c axis and a-b plane (ref 51) are graphically presented in the following figure 2.8.1. On average the Homes' constant calculated from data exceeds the Homes' constant derived from Trisine geometry by 1.72. There may be some degrees of freedom considerations $1 \cdot k_b T_c / 2$, $2 \cdot k_b T_c / 2$, $3 \cdot k_b T_c / 2$ that warrant looking into that may account for this divergence although conformity is noteworthy. Also 1.72 is close to sqrt(3), a value that is inherent to Trisine geometry. I will have to give this a closer look. In general, the conventional and high temperature superconductor data falls in the same pattern. I

Under the geometric scenario for superconducting materials presented herein, the Cooper CPT Charge conjugated pair centers of mass and centers of rotation(r) are different making the numerical results in table 2.9.1 valid. Under this scenario, it is the superconducting material that loses weight. The experimentally observed superconducting shielding effect cannot be explained in these terms.

2.10 BCS VERIFYING CONSTANTS

Equations 2.9.1 - 2.9.8 represent constants as derived from BCS theory [2] and considered by Little [4] to be primary constraints on any model depicting the superconducting phenomenon. It can be seen that the trisine model constants compare very favorably with BCS constants in brackets { }.

$$C_D = 10.2D(\epsilon_T)k_b^2T_c \frac{\mathbb{C}}{\text{cavity}} = 10.2k_b \frac{\mathbb{C}}{\text{cavity}} \quad (2.10.1)$$

$$\gamma = \frac{2}{3}\pi^2 D(\epsilon_T)k_b^2 \frac{\mathbb{C}}{\text{cavity}} = \frac{2}{3} \frac{\pi^2 k_b}{T_c} \frac{\mathbb{C}}{\text{cavity}} \quad (2.10.2)$$

$$\frac{1}{\mathbb{C}} \frac{\gamma T_c^2}{H_c^2} = .178 \left\{ \frac{\pi}{18} \text{ or } .170 \right\} \quad (2.10.3)$$

$$\frac{C_D}{\gamma T_c} = \frac{3 \cdot \text{jump}}{2\pi^2} \{1.52\} = 1.55 \{1.52\} \quad (2.10.4)$$

$$\frac{\hbar^2 \left(\frac{K_A^2}{\mathbb{C}} - K_{Dn}^2 \right)}{2m_i k_b T_c} = \text{jump} \{10.2\} \quad (2.10.5)$$

$$= 10.14 \{10.2\}$$

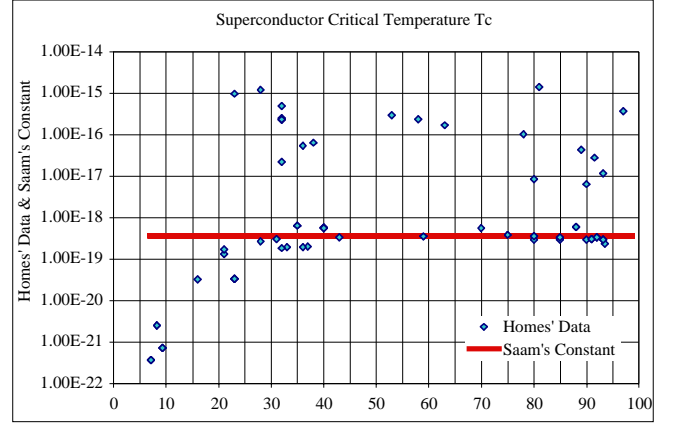
$$T_c^{\frac{3}{2}} \text{cavity} = \frac{3\pi^3 \hbar^3}{6^{\frac{1}{2}} m_i^{\frac{3}{2}} \left(\frac{B}{A} \right)_i k_b^{\frac{3}{2}}} \quad (2.10.6)$$

$$= 3.6196 \times 10^{-19} \quad (\text{Saam's Constant})$$

This equation basically assumes the ideal gas law for superconducting charge carriers. When the $1/\rho_s$ data from reference [51, 59] is used as a measure of cavity volume in the equation 2.10.6, the following plot is achieved. It is a good fit for some of the data and not for others. One can only conclude that the number of charge carriers in the cavity volume varies considerably from one superconductor to

another with perhaps only the Cooper CPT Charge conjugated pair being a small fraction of the total. Also, degrees of freedom may be a factor as in the kinetic theory of gas or other words – is a particular superconductor one, two or three dimensional ($1 \cdot k_b T_c / 2$, $2 \cdot k_b T_c / 2$, $3 \cdot k_b T_c / 2$) as Table 2.6.1 data for MgB_2 would imply? Also it is important to remember that Homes' data is from just above T_c and not at or below T_c .

Figure 2.10.1 Homes' Data Compared to Saam's Constant



$$\frac{\gamma T_c \text{cavity}}{k_b \mathbb{C}} = \left\{ \frac{2\pi^2}{3} \right\} \quad (2.10.7)$$

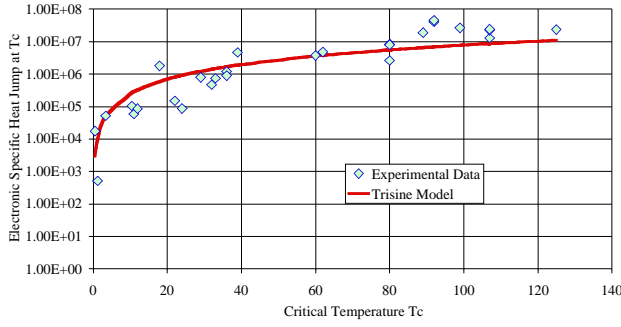
$$\frac{2\Delta_o^{BCS}}{k_b T_c} = 2\pi e^{-Euler} \{3.527754\} \quad (2.10.8)$$

Table 2.10.1 Electronic Heat Jump $k_b \mathbb{C} / \text{cavity}$ at T_c

T_c ($^{\circ}K$)	3,100,000	2,135	1,190	447	93	8.11E-16
T_c ($^{\circ}K$)	1.29E+11	3.38E+09	2.52E+09	1.55E+09	7.05E+08	2.729
$\frac{k_b \mathbb{C}}{\text{cavity}} \left(\frac{\text{erg}}{\text{cm}^3} \right)$	4.20E+13	7.59E+08	3.16E+08	7.28E+07	6.90E+06	1.78E-19

Harshman [17] has compiled and reported an extended listing of electronic specific heat jump at T_c data for a number of superconducting materials. This data is reported in units of $\text{mJ}/\text{mole } K^2$. With the volume per formula weight data for the superconductors also reported by Harshman and after multiplying by T_c^2 , the specific heat jump at T_c is expressed in terms of erg/cm^3 and graphed in figure 2.10.2.

Figure 2.10.2 Electronic Specific Heat Jump (C_d) at T_c comparing Harshman compiled experimental data and predicted trisine values based on equation 2.10.1



2.11 SUPERCONDUCTING COSMOLOGICAL CONSTANT

The following relations of $radius(R_U)$, $mass(M_U)$, $density(\rho_U)$ and $time(T_U)$ in terms of the superconducting *cosmological constant* are in general agreement with known data. This could be significant. The cosmological constant as presented in equation 2.11.1 is based on energy/area or *universe surface tension* (σ_U), as well as energy/volume or *universe pressure* (p_U). The *universe surface tension* (σ_U) is independent of (T_c) while the *universe pressure* (p_U) is the value at current CMBR temperature of $2.71^\circ K$ as presented in table 2.7.1 and observed by COBE [26] and later satellites. The *cosmological constant* also reduces to an expression relating trisine relativistic velocity transformed mass (m_t) the gravitational constant (G) and Planck's constant (\hbar). Also a reasonable value of 71.2km/sec-million parsec for the Hubble constant (H_U) from equation 2.11.13 is achieved based on a *universe absolute viscosity* (μ_U) and *energy dissipation rate* (P_U).

$$\text{cosmological constant} = \left\{ \begin{array}{l} \frac{16\pi G}{v_{dx}^4} \sigma_U \\ \frac{H_U}{\sqrt{3}c} \\ \frac{4}{\sqrt{3}\pi} \frac{m_t^3 G}{\hbar^2} \end{array} \right\} \quad (2.11.1)$$

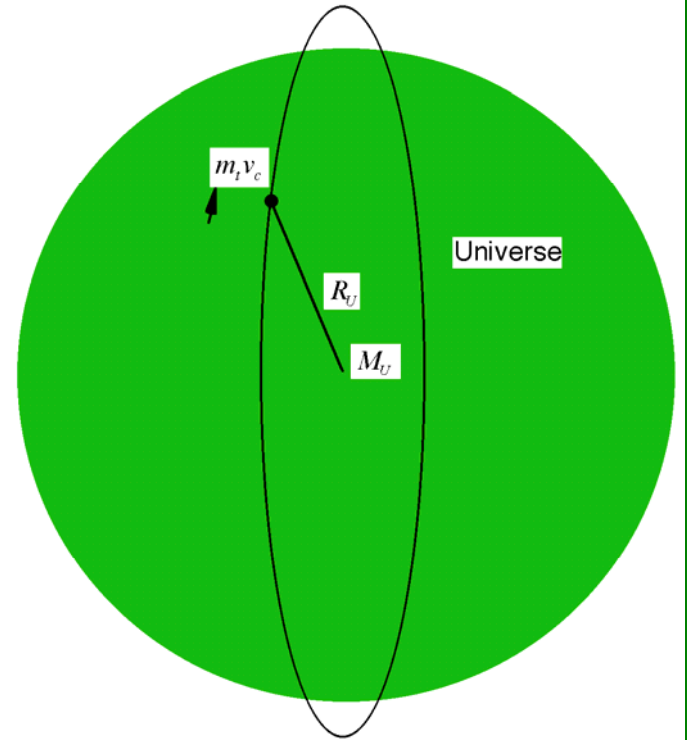
$$\sigma_U = \frac{C k_b T_c}{\text{section}} \quad (2.11.2)$$

$$R_U = \frac{1}{\text{cosmological constant}} \quad (2.11.3)$$

$$R_U = 2.25E+28 \text{ cm}$$

The mass of the universe (M_U) is established by assuming a spherical isotropic universe (center of mass in the universe center) of radius (R_U) such that a particle with the speed of light cannot escape from it as expressed in equation 2.11.4 and graphically described in figure 2.11.1.

Figure 2.11.1 Closed Universe with Mass M_U and Radius R_U



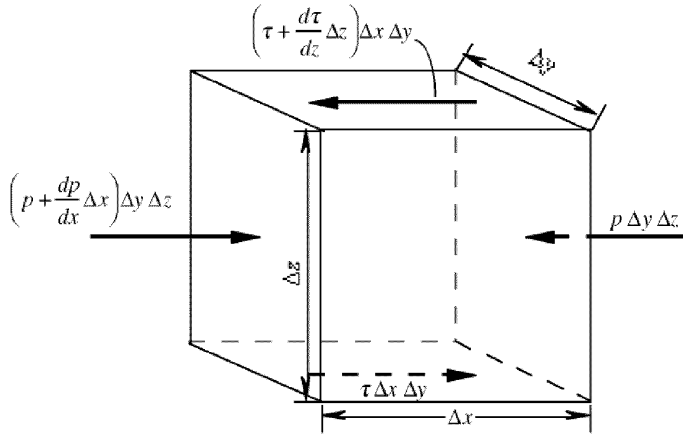
$$\begin{aligned} M_U &= R_U \cdot \frac{c^2}{G} \\ &= \frac{\sqrt{3}\pi}{4} \frac{\hbar^2 c^2}{m_t^3 G^2} \\ &= 3.02E+56 \text{ g} \end{aligned} \quad (2.11.4)$$

$$\begin{aligned}
\rho_U &= M_U \cdot \frac{3}{4\pi R_U^3} & (2.11.5) \\
&= \frac{4}{\pi^3} \frac{m_t^6 c^2 G}{\hbar^4} \\
&= \frac{m_t}{\text{cavity}} \Big|_{\substack{T_e=8.11E-16 \\ T_b=2.729}} \\
&= 6.38E-30 \text{ g/cm}^3
\end{aligned}$$

This value for Universe density is much greater than the density of the universe calculated from observed celestial objects. As reported in reference [27], standard cosmology model allows accurate determination of the universe baryon density of between $1.7E-31$ to $4.1E-31$ g/cm^3 . These values are 2.7 - 6.4% of the universe density reported herein based the background universe as superconductor.

$$\begin{aligned}
\text{Universe time}(T_U) &= \frac{R_U}{\sqrt{3}c} & (2.11.6) \\
&= \frac{\pi}{4} \frac{\hbar^2}{m_t^3 c G} \\
&= 4.32E+17 \text{ sec} \\
&\text{or } 1.37E+10 \text{ years}
\end{aligned}$$

Figure 2.11.2 Shear forces along parallel planes of an elemental volume of fluid



As illustrated in Figure 2.11.2 equation 2.11.13 for the Hubble constant (H_U) is derived by equating the forces acting on a cube of fluid in shear in one direction to those in the opposite direction, or

$$\begin{aligned}
p_U \Delta y \Delta z + \left[\tau + \frac{d\tau}{dz} \Delta z \right] \Delta x \Delta y & & (2.11.7) \\
= \tau \Delta x \Delta y + \left[p_U + \frac{dp_U}{dx} \Delta x \right] \Delta y \Delta z
\end{aligned}$$

Here p_U is the universe pressure intensity, τ the shear intensity, and Δx , Δy , and Δz are the dimensions of the cube. It follows that:

$$\frac{d\tau}{dz} = \frac{dp_U}{dx} \quad (2.11.8)$$

The power expended, or the rate at which work is done by the couple ($\tau \Delta x \Delta y$), equals the torque ($\tau \Delta x \Delta y$) Δz times the angular velocity dv/dz . Hence the universe power (P_U) consumption per universe volume (V_U) of fluid is

$$P_U/V_U = [(\tau \Delta x \Delta y) \Delta z \, dv/dz] / (\Delta x \Delta y \Delta z) = \tau \, (dv/dz).$$

$$\text{Defining} \quad \tau = \mu_U \, dv/dz$$

$$\text{and} \quad H_U = dv/dz$$

$$\text{then} \quad P_U/V_U = \mu_U \, (dv/dz)^2 = \mu_U H_U^2$$

$$\text{or} \quad H_U^2 = P_U / (\mu_U V_U)$$

The *universe absolute viscosity* (μ_U) is based on momentum/surface area as an outcome of classical kinetic theory of gas viscosity [19]. In terms of our development, the momentum changes over sectional area in each *cavity* such that:

$$\mu_U = \frac{m_t v_{dx}}{\text{section}} \quad (2.11.9)$$

Derivation of the kinematic viscosity (ν_U) in terms of absolute viscosity as typically presented in fluid mechanics [18], a constant universe kinematic viscosity (ν_U) is achieved in terms of Planck's constant (\hbar) and Cooper CPT Charge conjugated pair relativistic velocity transformed mass (m_t).

$$\begin{aligned}
\nu_U &= \frac{\text{cavity}}{m_t} \mu_U & (2.11.10) \\
&= \pi \frac{\hbar}{m_t} \frac{A}{B} \\
&= 1.39E-02 \frac{\text{cm}^2}{\text{sec}}
\end{aligned}$$

Derivation of the Universe Energy Dissipation Rate (P_U) assumes that all of the universe mass (M_U) is in the superconducting state. In other words, our visible universe

contributes an insignificant amount of mass to the universe mass. This assumption appears to be valid due to the subsequent calculation of the Hubble constant (H_U) of 71.2km/sec-million parsec (equation 2.11.13) which falls within the experimentally observed value[20] on the order of 70-80 km/sec-million parsec and the recently measured 70 km/sec-million parsec within 10% as measured by a NASA Hubble Space Telescope Key Project Team on May 25, 1999 after analysis of 800 Cepheid stars, in 18 galaxies, as far away as 65 million light years.

$$P_U = \frac{M_U v_{dx}^2 v_{dx}}{2 R_U} \quad (2.11.11)$$

$$\begin{aligned} \text{Universe volume}(V_U) &= \frac{4}{3} \pi R_U^3 & (2.11.12) \\ &= \frac{\sqrt{3} \pi^4 \hbar^6}{16 m_i^9 G^3} \\ &= 4.74E + 85 \text{ cm}^3 \end{aligned}$$

$$\begin{aligned} H_U &= \sqrt{\frac{P_U}{\mu_U V_U}} & (2.11.13) \\ &= \frac{4 m_i^3 G c}{\pi \hbar^2} \\ &= 2.31E - 18 / \text{sec} \end{aligned}$$

or in more conventionally reported units:

$$H_U = 71.23 \frac{\text{km}}{\text{sec}} \frac{1}{\text{million parsec}}$$

Now from equation 2.11.1 and 2.11.13 the *cosmological constant* is defined in terms of the Hubble constant (H_U) in equation 2.11.14.

$$\begin{aligned} \text{Cosmological constant} &= \frac{H_U}{\sqrt{3}c} & (2.11.14) \\ &= \frac{1}{R_U} \\ &= 4.45E-29 \text{ cm}^{-1} \end{aligned}$$

Now from equation 2.11.4 and 2.11.13 the *universe mass* (M_U) is defined in terms of the Hubble constant (H_U) in equation 2.11.15.

$$\begin{aligned} M_U &= \frac{\sqrt{3}c^3}{H_U G} & (2.11.15) \\ &= \frac{\sqrt{3} \pi \hbar^2 c^2}{4 m_i^3 G^2} \\ &= \frac{R_U c^2}{G} \\ &= 3.02E56 \text{ g} \end{aligned}$$

Now from equation 2.11.13 and 2.11.5 the *universe density* (ρ_U) is defined in terms of the Hubble constant (H_U) in equation 2.11.16. This differs from the universe critical density equation in reference [27] by a factor of 2/3 which indicates an inflationary universe.

$$\begin{aligned} \rho_U &= \frac{2 H_U^2}{8 \pi G} = \frac{3 \text{ chain } H_U^2}{8 \pi \text{ cavity } G} & (2.11.16) \\ &= 6.38E - 30 \frac{\text{g}}{\text{cm}^3} \end{aligned}$$

Now from equation 2.11.13 and 2.11.6 the *universe time* (T_U) is defined in terms of the Hubble constant (H_U) in equation 2.11.17.

$$\begin{aligned} T_U &= \frac{1}{H_U} & (2.11.17) \\ &= 4.32E+17 \\ &\text{or } 1.37E10 \text{ years} \end{aligned}$$

$$\text{Universe mass creation rate}(\dot{M}_U) = \frac{P_U}{c^2} \quad (2.11.18)$$

Table 2.11.1 Vacuum parameters

T_c ($^{\circ}K$)	3,100,000	2,135	1,190	447	93	8.1E-16
T_b ($^{\circ}K$)	1.3E+11	3.4E+09	2.5E+09	1.6E+09	7.1E+08	2.729
μ_U (g/cm/sec)	2.09E+01	3.78E-04	1.57E-04	3.62E-05	3.44E-06	8.85E-32
σ_U (erg/cm ²)	5.02E+11	2.38E+05	7.40E+04	1.04E+04	4.52E+02	3.43E-32
P_U (erg/sec)	5.31E+51	9.59E+46	3.99E+46	9.19E+45	8.72E+44	2.24E+19
\dot{M}_U (g/sec)	5.91E+30	1.07E+26	4.44E+25	1.02E+25	9.70E+23	2.50E-02

This development would allow the galactic collision rate calculation in terms of the Hubble constant (H_U) (which is considered a shear rate in our fluid mechanical concept of the universe) in accordance with the Smolukowski relationship [12, 13, 14] where J_U represents the collision rate of galaxies of two number concentrations (n_i, n_j) and diameters (d_i, d_j):

$$J_U = \frac{1}{6} n_i n_j H_U (d_i + d_j)^3 \quad (2.11.19)$$

The superconducting Reynolds' number (R_e), which is defined as the ratio of inertial forces to viscous forces is presented in equation 2.11.20 and has the value of one(1). In terms of conventional fluid mechanics this would indicate a condition of laminar flow [18].

$$\begin{aligned} R_e &= \frac{m_t}{cavity} v_{dx} \frac{1}{section \mu} \quad (2.11.20) \\ &= \frac{m_t v_{dx}}{\mu section} \\ &= 1 \end{aligned}$$

$$\begin{aligned} a_U &= \pi e^{-Euler} \left(\frac{v_{dx}^2}{2P} \right) \Bigg|_{T_c=8.11E-16}^{T_b=2.729} \quad (2.11.21) \\ &= cH_U = \sqrt{\frac{P_U c^2}{\mu_U V_U}} \\ &= 6.93 \times 10^{-8} \frac{cm}{sec^2} \end{aligned}$$

The numerical value of the universal deceleration (a_U) expressed in equation 2.11.21 is nearly equal to that observed with Pioneer 10 & 11 [53], but this near equality is viewed as coincidence only. This acceleration component of the universal dark matter/energy may provide the mechanism for observed universe expansion and primarily at the boundary of the elastic space CPT lattice and Baryonic matter (star systems, galaxies, etc).

2.12 SUPERCONDUCTING VARIANCE AT T/Tc

Establish Gap and Critical Fields as a Function of T/T_c

Using Statistical Mechanics [19]

$$z_s = e^{\frac{-h^2 K_B^2 chain}{2m_e k_b T_c cavity}} = e^{-\frac{2}{3}} \quad (2.12.1)$$

$$cavity = \frac{3\pi^3 \hbar^3}{6^2 m_t^2 \left(\frac{B}{A}\right)_t k_b^2 T_c^2} \quad (2.12.2)$$

$$z_t = \frac{(2\pi m_t k_b T_c)^{\frac{3}{2}} cavity^{1.3\%}}{8\pi^3 \hbar^3} \approx \left(\frac{T}{T_c}\right)^{\frac{3}{2}} \quad (2.12.3)$$

$$k_t = \frac{z_t}{z_s} e^{\frac{k_b T_c}{k_b T}} = \left(\frac{T}{T_c}\right)^{\frac{3}{2}} e^{\frac{2}{3}} e^{-\frac{T_c}{T}} = \left(\frac{T}{T_c}\right)^{\frac{3}{2}} e^{\left(\frac{2}{3} - \frac{T_c}{T}\right)} \quad (2.12.4)$$

$$k_s = \frac{2}{3} - k_t = \frac{chain}{cavity} - k_t \quad (2.12.5)$$

$$\Delta_r = 1 - \frac{1}{3} \frac{T}{T_c} \frac{1}{\ln\left(\frac{1}{k_t}\right)} = 1 + \frac{1}{3} \frac{T}{T_c} \frac{1}{\ln(k_t)} \quad (2.12.6)$$

$$H_{T1}^2 = H_o^2 \left[1 - \frac{2}{3} \pi^2 \left(\frac{T}{\pi e^{-Euler} T_c} \right)^2 \right] \quad (2.12.7)$$

$$\text{at } \frac{T}{T_c} \text{ near } 0$$

$$H_{T2}^2 = H_o^2 k_s \quad \text{at } \frac{T}{T_c} \text{ near } 1 \quad (2.12.8)$$

$$Avg H_{cT}^2 = \left[\begin{array}{l} \text{if } H_{cT1}^2 > H_{cT2}^2 \\ \text{then } H_{cT1}^2 \text{ else } H_{cT2}^2 \end{array} \right] \quad (2.12.9)$$

2.13 SUPERCONDUCTOR ENERGY CONTENT

Table 2.13.1 presents predictions of superconductivity energy content in various units that may be useful in anticipating the uses of these materials.

Table 2.13.1 Superconductor Energy in Various Units.

T_c ($^{\circ}K$)	3,100,000	2,135	1,190	447	93	8.1E-16
T_s ($^{\circ}K$)	1.3E+11	3.4E+09	2.5E+09	1.6E+09	7.1E+08	2.729
erg/cm ³	1.61E+20	2.00E+12	4.64E+11	4.01E+10	7.92E+08	1.78E-34
joule/liter	1.61E+16	2.00E+08	4.64E+07	4.01E+06	7.92E+04	1.78E-38
BTU/ft ³	4.32E+14	5.37E+06	1.25E+06	1.08E+05	2.13E+03	4.77E-40
kwhr/ft ³	1.26E+11	1.57E+03	3.65E+02	3.16E+01	6.23E-01	1.40E-43
kwhr/gallon	2.27E+10	2.82E+02	6.54E+01	5.66E+00	1.12E-01	2.51E-44
gasoline equivalent	3.46E+08	4.30E+00	1.00	8.63E-02	1.70E-03	3.82E-46

Table 2.13.2 represents energy level of trisine energy states and would be key indicators material superconductor

characteristics at a particular critical temperature. The BCS gap is presented as a reference energy.

Table 2.13.2 Energy (ev) associated with Various Trisine Wave Vectors. The energy is computed by $(\hbar^2/2m_i)K^2$ and expressing as electron volts(ev). The BCS gap is computed as $(\pi/\exp(Euler))(\hbar^2/2m_i)K_B^2$.

$T_c (^{\circ}K)$	3,100,000	2,135	1,190	447	93	8.1E-16
$T_b (^{\circ}K)$	1.3E+11	3.4E+09	2.5E+09	1.6E+09	7.1E+08	2.729
K_B^2	2.67E+02	1.84E-01	1.03E-01	3.85E-02	8.01E-03	6.99E-20
K_C^2	8.96E+02	6.17E-01	3.44E-01	1.29E-01	2.69E-02	2.34E-19
K_{Ds}^2	8.32E+02	5.73E-01	3.19E-01	1.20E-01	2.50E-02	2.18E-19
K_{Dn}^2	3.20E+02	2.20E-01	1.23E-01	4.62E-02	9.60E-03	8.37E-20
K_P^2	3.56E+02	2.45E-01	1.37E-01	5.14E-02	1.07E-02	9.31E-20
$K_{Ds}^2 + K_B^2$	1.10E+03	7.57E-01	4.22E-01	1.58E-01	3.30E-02	2.87E-19
$K_{Dn}^2 + K_B^2$	5.87E+02	4.04E-01	2.25E-01	8.47E-02	1.76E-02	1.54E-19
$K_{Ds}^2 + K_C^2$	1.73E+03	1.19E+00	6.63E-01	2.49E-01	5.18E-02	4.52E-19
$K_{Dn}^2 + K_C^2$	1.22E+03	8.38E-01	4.67E-01	1.75E-01	3.65E-02	3.18E-19
$K_{Ds}^2 + K_P^2$	1.19E+03	8.18E-01	4.56E-01	1.71E-01	3.56E-02	3.11E-19
$K_{Dn}^2 + K_P^2$	6.76E+02	4.66E-01	2.60E-01	9.75E-02	2.03E-02	1.77E-19
K_A^2	6.05E+03	4.17E+00	2.32E+00	8.72E-01	1.81E-01	1.58E-18
BCS gap	4.71E+02	3.25E-01	1.81E-01	6.79E-02	1.41E-02	1.23E-19

2.14 SUPERCONDUCTOR GRAVITATIONAL ENERGY

As per reference[25], a spinning nonaxisymmetric object rotating about its minor axis with angular velocity ω will radiate gravitational energy in accordance with equation 2.14.1

$$\dot{E}_g = \frac{32G}{5c^5} I_3^2 \zeta^2 \omega^6 \quad (2.14.1)$$

This expression has been derived based on weak field theory assuming that the object has three principal moments of inertia I_1, I_2, I_3 , respectively, about three principal axes $a > b > c$ and ζ is the ellipticity in the equatorial plane.

$$\zeta = \frac{a-b}{\sqrt{ab}} \quad (2.14.2)$$

Equations 2.14.1 with 2.14.2 were developed for predicting

gravitational energy emitted from pulsars but we use them to calculate the gravitational energy emitted from rotating Cooper CPT Charge conjugated pairs in the trisine superconducting mode.

Assuming the three primary trisine axes $C > B > A$ corresponding to $a > b > c$ in reference [25] as presented above, then the trisine ellipticity would be:

$$\zeta = \frac{C-B}{\sqrt{CB}} = 1 \quad (2.14.3)$$

Assuming a mass (m_s) with density (ρ) containing superconducting pairs with density (ρ_c) rotating around a nonaxisymmetric axis of relativistic radius B to establish moment of inertia (I_3) then equation 2.14.1 becomes:

$$\dot{E}_g = \frac{32G}{5c^5} \left(m_s \frac{\rho_c}{\rho} B^2 \right)^2 \omega^6 \quad (2.14.4)$$

Then integrating with respect to time where $\omega = 2\pi/\text{time}$, and replacing speed of light (c) with De Broglie speed of light (v_{dx}), then equation 2.14.4 becomes:

$$\begin{aligned} E_g &= -\frac{32G}{5v_{dx}^5} \left(m_s \frac{\rho_c}{\rho} B^2 \right)^2 \frac{6(2\pi)^6}{\text{time}^5} \\ &= -\frac{384\pi^6}{5} G \frac{\rho_c^2 m_s^2}{\rho^2 B} \end{aligned} \quad (2.14.5)$$

In the Podkletnov experiment [7], 5.47834 gram silicon dioxide disc was weighed over a rotating superconducting disk 145 mm in diameter and 6 mm in thickness with a mass (m) of 633 grams based on a $YBa_2Cu_2O_{6.95}$ density of 6.33 g/cm^3 . Based on equation 2.14.5 the gravitation energy associated with this superconducting material would be -46.1 ergs as indicated in table 2.14.1. Assuming this energy is reflected in gravitational potential energy in regards to the weighed silicon dioxide mass, then it can be reflected in a weight loss of .05% at 17 cm or in other words the relationship in equation 2.14.6 holds.

$$\begin{aligned} -mgh &= -.0005 \cdot 5.48 \text{ g} \cdot 980 \frac{\text{cm}}{\text{sec}^2} \cdot 17 \text{ cm} \\ &= -45.5 \text{ erg} \end{aligned} \quad (2.14.6)$$

In the Podkletnov experiment [7], the .05% weight loss was observed with the silicon dioxide weight at 1.5 cm above the superconducting mass (m_s). The size of the silicon dioxide

mass is not given by Podkletnov but with a weight of 5.47834 grams, its projected area onto the superconducting mass must be only a few square centimeters compared to the area of the superconducting disc of $\pi 14.5^2$ or 660 cm^2 . These relative area's may have something to do with the less observed weight loss relative to what is predicted based on relative masses alone.

Table 2.14.1

$T_c (^{\circ}K)$	3,100,000	2,135	1,190	447	93	8.1E-16
$T_b (^{\circ}K)$	1.3E+11	3.4E+09	2.5E+09	1.6E+09	7.1E+08	2.729
$-E_g$ (-erg)	-3.1E+17	-2.6E+06	-3.4E+05	-1.1E+04	-4.6E+01	-8.9E-59

All of this is consistent with the Virial Theorem for a system of particles with total mass M.

Gravitational Potential Energy = Kinetic Energy

$$\frac{1}{2} Gm_t^2 \frac{3}{\Delta x + \Delta y + \Delta z} \Big|_{\substack{T_c=8.11E-16 \\ T_b=2.729}} = \frac{1}{2} m_r v_{dx}^2 \Big|_{\substack{T_c=8.11E-16 \\ T_b=2.729}} \quad (2.14.7)$$

Also:

$$\left\{ \begin{array}{l} \frac{1}{2\epsilon_x k_m} m_t v_{dx}^2 \Big|_{\substack{T_c=8.11E-16 \\ T_b=2.729}} \\ \frac{\text{chain}}{\text{cavity}} \frac{1}{2\epsilon_x k_m} \frac{1}{\epsilon} \frac{e^2}{B} \Big|_{\substack{T_c=8.11E-16 \\ T_b=2.729}} \end{array} \right\} = \frac{1}{2} m_r v_{dx}^2 \Big|_{\substack{T_c=8.11E-16 \\ T_b=2.729}}$$

where : (2.14.7a)

$$2\epsilon_x k_m = \frac{2c^2}{v_{dx}^2} = \frac{1}{1 - \sqrt{1 - \frac{v_{dx}^2}{c^2}}} \Big|_{\substack{T_c=8.11E-16 \\ T_b=2.729}}$$

Where m_t and m_r are related as in Equation 2.1.25 and $\Delta x, \Delta y, \Delta z$ are Heisenberg Uncertainties as expressed in equation 2.1.20.

In the case of a superconductor, the radius R is the radius of curvature for pseudo particles described in this report as the variable B. All of the superconductor pseudo particles move in asymmetric unison, making this virial equation applicable to this particular engineered superconducting situation. This is consistent with Misner Gravitation [35] page 978 where it is

indicated that gravitational power output is related to “power flowing from one side of a system to the other” carefully incorporating “only those internal power flows with a time-changing quadrupole moment”. The assumption in this report is that a super current flowing through a trisine superconducting CPT lattice has the appropriate quadrupole moment at the dimensional level of B. The key maybe a linear back and forth trisine system. Circular superconducting systems such as represented by Gravity Probe B gyroscopic elements indicate the non gravitational radiation characteristic of such circular systems reinforcing the null results of mechanical gyroscopes [21, 22, 23].

3. DISCUSSION

This effort is towards formulating of a theoretical frame work towards explaining the Podkletnov's and Nieminen's results but in the process, relationships between electron/proton mass, charge and gravitational forces were established which appear to be unified under this theory with links to the cosmological constant, the dark matter of the universe, and the universe black body radiation as a relic of its big bang origins.

The overall theory is an extension to what Sir Arthur Eddington proposed during the early part of this century. He attempted to relate proton and electron mass to the number of particles in the universe and the universe radius. Central to his approach was the fine structure constant ($\hbar c/e^2$), which is approximately equal to 137. This relationship is also found as a consequence of our development in equation 2.1.16, the difference being that a material dielectric(ϵ) modified velocity of light(v_e) is used. To determine this dielectric(v_e), displacement(D) and electric fields(E) are determined for Cooper CPT Charge conjugated pairs moving through the trisine CPT lattice under conditions of the trisine CPT lattice diamagnetism equal to $-1/4\pi$ (the Meissner effect). Standard principles involving Gaussian surfaces are employed and in terms of this development the following relationship is developed based on equation 2.1.17 containing the constant ($\hbar c/e^2$) and relating electron mass(m_e), trisine relativistic velocity transformed mass (m_t) and the characteristic trisine geometric ratio(B/A).

$$\frac{1}{2} \frac{m_t^2}{m_e^2} g_e g_s = 4\pi 3^{-\frac{1}{4}} \left(\frac{\hbar c}{e^2} \right) \left(7 \frac{A^2}{B^2} + 12 \frac{B^2}{A^2} + 19 \right) \quad (3.1)$$

The extension postulated herein is that the principles expounded in 'twin paradox' in special relativity are

applicable to orbiting bodies at the microscopic level. In this case, charged particles move in symmetrical vortex patterns within a superconductor with velocity (v_e) allowed by the dielectric properties of the particular medium. As a result, a time dilation ($time_{_}$) is generated between this frame of reference and the stationary frame of reference. This transform also results in increase in relativistic mass (m_r). The trisine symmetry of the medium then allows pseudo particles (Cooper CPT Charge conjugated pairs) with relativistic mass (m_r) to move with a corresponding De Broglie velocity (v_{dx}), which expresses itself in a super current (J).

At this time, it is not known whether the trisine CPT lattice is the only Gaussian surface, which would provide such results, but it may be so.

Also, it is important to note, that the trisine surface may or may not relate to any physical structure in a superconducting material. Although this is so, this theory may provide a basis for a "jump" in thinking from material with T_c 's below 100 degree Kelvin to required anticipated materials with T_c 's on the order of 1000's of degrees Kelvin.

The present theory predicts the .05% weight loss of the 93 degree Kelvin superconducting material in earth's gravitational field. The presented theory is based on theory developed for predicting gravitational radiation from celestial objects.

In concert with the weight loss prediction, it is also indicated that the superconducting material itself will loose .05% of it weight.

The implications of such a verified effect are profound. Conditions could be postulated as in table 2.9.1, such that a mass could be rendered weightless in earth's gravity. Podkletnov and Nieminen alluded to the basic mechanism developed in this report, in that a spinning mass develops its own gravity as depicted in Figure 2.9.1 although it must be noted that the center of rotation must differ from the center of mass (nonaxisymmetric spinning) as is the case with the superconducting theory presented herein. Also, it is noted that if somehow the Cooper CPT Charge conjugated pairs could be separated from the material, the gravitational force shielding effect would be much more pronounced or in other words the lower superconducting material density (approaching the Cooper CPT Charge conjugated pair density) the greater the effect.

It is important to note also that the Cooper CPT Charge conjugated pairs are postulated to travel along a radius of curvature (B) with tangential velocity (v_{dt}) and not in a circle

or in other words the Cooper CPT Charge conjugated pairs center of masses differs from their center of rotation. This velocity (v_{dt}) is in three dimensions and the vector sum of x, y and z components. This means that no matter what the orientation of the superconducting material, there will be a tangential velocity vector facing the center of the earth as indicated in Figure 2.9.1. In other words, as the earth rotates, there will be a tangential component in the superconductor circular to the earth's axis as defined by a line from the earth's center to the center of rotation of the Cooper CPT Charge conjugated pairs with a constant gravitational force shielding effect.

Also, it is evident from the gravitation shielding principle graphically presented in figure 6, that it does not matter what forces hold the rotating mass in orbit whether they be magnetic, electrical or mechanical. The orbit retaining mechanism postulated in this report is electrical and magnetic.

Also, without quantitative calculations, it is easy to postulate that a spinning superconducting disc would add to the inherent tangential velocity (v_{dt}) of the superconductor and therefore provide an amplifying effect to the lessening of weight and to the experimentally observe shielding effect.

As of this time, it is noted that the results of Podkletnov have not been independently verified. It is thought that the reason is that a pure $YBa_2Cu_3O_{7-x}$ superconductor having the theoretically possible super currents is not easily fabricated. Perhaps Podkletnov is the only one who knows how to do this at this time.

4. CONCLUSION

A momentum and energy conserving (elastic) CPT lattice called trisine and associated superconducting theory is postulated whereby electromagnetic and gravitational forces are mediated by a particle of relativistic velocity transformed mass (110.123 x electron mass) such that the established electron/proton mass is maintained, electron and proton charge is maintained and the universe radius as computed from Einstein's cosmological constant is 2.25E28 cm, the universe mass is 3.0E56 gram, the universe density is 6.38E-30 g/cm³ and the universe time is 1.37E10 years.

The cosmological constant is based on a universe surface tension directly computed from a superconducting energy over surface area.

The calculated universe mass and density are based on an

isotropic homogeneous media filling the vacuum of space analogous to the 'aether' referred to in the 19th century (but still in conformance with Einstein's relativity theory) and could be considered a candidate for the 'cold dark matter' in present universe theories. Universe density is 2/3 of conventionally calculated critical density. This is in conformance with currently accepted inflationary state of the universe.

The 'cold dark matter' emits a CMBR of $2.729^\circ K$ as has been observed by COBE and later satellites although its temperature in terms of superconducting critical temperature is an extremely cold $8.11E-16^\circ K$.

Also, the recently reported results by Podkletnov and Nieminen wherein the weight of an object is lessened by .05% are theoretically confirmed where the object is the superconductor, although the gravitational shielding phenomenon of $YBa_2Cu_3O_{7-x}$ is yet to be explained. In future experiments, the weight of the superconducting object should be measured. It is understood that the Podkletnov and Nieminen experiments have not been replicated at this time. It could be that the very high super currents that are required have not been replicated from original experiment. The model herein interprets the Podkletnov experimental data in the context of the virial theorem to which a particular superconductor must be engineered.

The trisine model provides a basis for considering the phenomenon of superconductivity in terms of an ideal gas with 1, 2 or 3 dimensions. The trisine model was developed primarily in terms of 1 dimension, but experimental data from MgB_2 would indicate a direct translation to 3 dimensions.

Also dimensional guidelines are provided for design of room temperature superconductors and beyond. These dimensional scaling guidelines have been verified by Homes' Law and generally fit within the conventionally described superconductor operating in the "dirty" limit. [54]

The deceleration observed by Pioneer 10 & 11 as they exited the solar system into deep space appear to verify the existence of an space energy density consistent with the amount theoretically presented in this report. This translational deceleration is independent of the spacecraft velocity and indicates that our solar system is comoving with a surrounding or supporting uniform energy or mass density. Also, the same space density explains the Pioneer spacecraft rotational deceleration. This is remarkable in that translational and rotational velocities differ by three (3) orders of magnitude.

General conclusions from study of Pioneer deceleration data are itemized as follows:

1. Dark Matter and Dark Energy are the same thing and are represented by a Trisine Elastic Space CPT lattice which is composed of virtual particles adjacent Heisenberg Uncertainty
2. Dark Matter and Dark Energy are related to Cosmic Microwave Background Radiation (CMBR) through very large space dielectric (permittivity) and permeability constants.
3. A very large Trisine dielectric constant and CPT equivalence makes the Dark Matter/Energy invisible to electromagnetic radiation.
4. A velocity independent ($v \ll c$) drag force acts on all objects passing through the Trisine Space CPT lattice and models the translational and rotational deceleration of Pioneer 10 & 11 space craft.
5. The Asteroid Belt marks the interface between solar wind and Trisine, the radial extent an indication of the dynamics of the energetic interplay of these two fields
6. The Trisine Model predicts no Dust in the Kuiper Belt. The Kuiper Belt is made of large Asteroid like objects.
7. The observed Matter Clumping in Galaxies is due to magnetic or electrical energetics in these particular areas at such a level as to destroy the Coherent Trisine.
8. The observed Universe Expansion is due to Trisine Space CPT lattice internal pressure.
9. When the Trisine is scaled to molecular dimensions, superconductor parameters such as critical fields, penetration depths, coherence lengths, Cooper CPT Charge conjugated pair densities are modeled.
10. A superconductor is considered electrically neutral with balanced conjugated charge as per CPT theorem. Observed current flow is due to one CPT time frame being pinned relative to observer.

A question logically develops from this line of thinking and that is "What is the source of the energy or mass density?". After the energy is imparted to the spacecraft passing through space, does the energy regenerate itself locally or essentially reduce the energy of universal field? And then there is the most vexing question based on the universal scaled superconductivity hypothesis developed in this report and that is whether this phenomenon could be engineered at an appropriate scale for beneficial use.

One concept for realizing this goal, is to engineer a wave crystal reactor. Ideally, such a wave crystal reactor would be

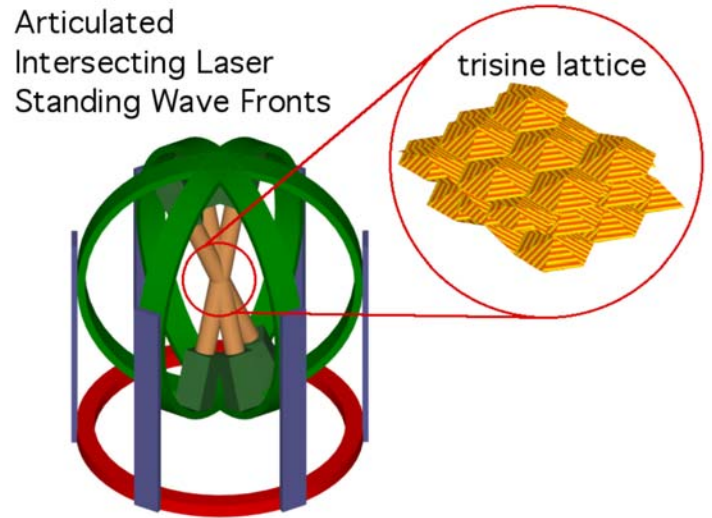
made in the microwave (cm wave length). Perhaps such microwaves would interact at the $\hbar\omega/2$ energy level in the Trisine CPT lattice pattern. Conceptually a device as indicated below may be appropriate where the green area represents reflecting, generating and polarizing surfaces of coherent electromagnetic radiation creating standing waves (in red zone) which interact in the intersecting zone defined by the trisine characteristic angle of $(90 - 22.8)$ degrees and 120 degrees of each other.

Figure 4.1 Conceptual Trisine Generator (Elastic Space CPT lattice)



The major conclusion of this report is that an interdisciplinary team effort is required to continue this effort involving physicists, chemists and engineers. Each has a major role in achieving the many goals that are offered if more complete understanding of the superconducting phenomenon is attained in order to bring to practical reality and bring a more complete understanding of our universe.

Figure 4.2 Conceptual Trisine Generator (Elastic Space CPT lattice) Within Articulating Motion Control Mechanism



5. VARIABLE AND CONSTANT DEFINITIONS

Fundamental Physical Constants are from National Institute of Standards (NIST).

name	symbol	value	units
Attractive Energy	V		$g\ cm^2\ sec^{-2}$
Boltzmann constant	k_b	1.380658120E-16	$g\ cm^2\ sec^{-2}\ Kelvin^{-1}$
Bohr magneton		9.27400949E-21	erg/gauss (gauss cm^3)
Bohr radius	a_o	5.2917724924E-09	cm
De Broglie velocity	$v_{dx}, v_{dy}, v_{dz}, v_{dT}$		cm sec^{-1}
Cooper CPT conjugated pair	©	2	unitless
correlation length	ξ		cm
critical magnetic fields	H_{c1}, H_{c2}, H_c		$g^{1/2}\ cm^{-1/2}\ sec^{-1}$
critical temperature	T_c		$^{\circ}K$
dielectric constant	ϵ		unitless
Dirac's number	g_d	1.001159652186	unitless
displacement & electric fields	D, E		$g^{1/2}\ cm^{-1/2}\ sec^{-1}$
electron mass	m_e	9.10938975E-28	g
earth radius	R_E	6.371315E+08	cm
earth mass	M_E	5.979E+27	g
relativistic mass	m_r		g
proton mass	m_p	1.67262311E-24	g
electron charge	e	4.803206799E-10	$cm^{3/2}\ g^{1/2}\ sec^{-1}$
electron gyromagnetic-factor	g_e	2.0023193043862	unitless
energy	E		$g\ cm^2\ sec^{-2}$
fluxoid	Φ	2.0678539884E-7	$g^{1/2}\ cm^{3/2}\ sec^{-1}$
fluxoid dielectric(ϵ) mod	Φ_{ϵ}		$g^{1/2}\ cm^{3/2}\ sec^{-1}$
gravitational constant	G	6.6725985E-8	$cm^3\ sec^{-2}\ g^{-1}$
London penetration depth	λ		cm
momentum vectors	P_x, P_y, P_z		$g\ cm^{-1}\ sec^{-1}$
natural log base	e	2.718281828459050	unitless
Planck's constant	$\hbar(h/2\pi)$	1.054572675E-27	$g\ cm^2\ sec^{-1}$
relativistic CPT time $_{\pm}$	$time_{\pm}$		second
superconductor gyro-factor	g_s	1.0096915	unitless
trisine angle	θ	22.80	angular degrees
trisine areas	<i>section, approach, side</i>		cm^2
trisine unit	<i>cell</i>		unitless
trisine constant	<i>trisine</i>	2.01091660	unitless

trisine density of states	$D(\epsilon_t)$		$\text{sec}^2 g^{-1} \text{cm}^{-2}$
trisine dimensions	A, B, C, P		cm
trisine mass	m_t	1.0031502157E-25	g
transformed mass	m_t	110.71029 x m_e	g
trisine size ratio	$(B/A)_t$	2.37933	<i>unitless</i>
trisine volume per cell	<i>cavity</i>		cm^3
trisine volume per chain	<i>chain</i>		cm^3
trisine wave vectors	$K_A, K_B, K_C, K_{Dn}, K_{Ds}$		cm^{-1}
universe absolute viscosity	μ_U		$g \text{ cm}^{-1} \text{ sec}^{-1}$
universe density	ρ_U	1.45E-29	$g \text{ cm}^{-3}$
universe kinematic viscosity	ν_U		$\text{cm}^2 \text{ sec}^{-1}$
universe radius	R_U	1.49E+28	cm
universe mass	M_E	2.01E+56	g
universe pressure	p_U		$g \text{ cm}^{-1} \text{ sec}^{-2}$
universe time	T_U		sec
velocity of light	c	2.997924580E+10	cm sec^{-1}
ϵ modified velocity of light	v_ϵ		cm sec^{-1}

APPENDIX A. TRISINE NUMBER AND B/A RATIO DERIVATION

BCS approach [2]

$$\Delta_o^{BCS} = \frac{\hbar\omega}{\sinh\left(\frac{1}{D(\epsilon_T)V}\right)} \quad (\text{A.1})$$

Kittel approach [4-Appendix H]

$$\Delta_o = \frac{2\hbar\omega}{e^{\frac{1}{D(\epsilon_T)V}} - 1} \quad (\text{A.2})$$

Let the following relationship where BCS (equation A.1) and Kittel (equation A.2) approach equal each other define a particular superconducting condition.

$$k_b T_c = \begin{cases} \frac{e^{Euler} \hbar\omega}{\pi \sinh\left(\frac{1}{D(\epsilon_T)V}\right)} \\ \frac{\hbar\omega}{e^{\frac{1}{D(\epsilon_T)V}} - 1} \end{cases} \quad (\text{A.3})$$

Define:

$$\frac{1}{D(\epsilon_T)V} = trisine \quad (\text{A.4})$$

Then:

$$trisine = -\ln\left(\frac{2e^{Euler}}{\pi} - 1\right) = 2.01091660 \quad (\text{A.5})$$

Given:

$$\frac{2m_t k_b T_c}{\hbar^2} = \begin{cases} \frac{(KK)_{\hbar\omega} e^{Euler}}{\pi \sinh(trisine)} \\ \frac{(KK)_{\hbar\omega}}{e^{trisine} - 1} \end{cases} = K_B^2 \quad (\text{A.6})$$

Ref: [2,4]

And within Conservation of Energy Constraint:

$$\left(\frac{m_p - m_e}{m_p}\right) \left(\frac{m_t - m_e}{m_t}\right) (K_B^2 + K_C^2) = (K_{D_s}^2 + K_{D_n}^2) \quad (\text{A.7})$$

And Within Conservation of Momentum Constraint:

$$\left(\frac{m_p}{m_p - m_e}\right) \left(\frac{m_t}{m_t - m_e}\right) (K_B + K_C) = (K_{D_s} + K_{D_n}) \quad (\text{A.8})$$

And from (KK) from table A.1:

$$(KK) = K_C^2 + K_{D_s}^2 \quad (\text{A.9})$$

Also from table A.1:

$$\frac{2\Delta_o^{BCS}}{k_b T_c} = \frac{2\pi}{e^{Euler}} = \frac{2K_{D_s}^{.065\%}}{K_B} \approx 3.527754 \quad (\text{A.10})$$

Also:

$$\frac{\Delta_o}{k_b T_c} = 2 \quad (\text{A.11})$$

Also from table A.1:

$$trisine = \frac{K_B^2 + K_P^2}{K_P K_B} \quad (\text{A.12})$$

Table A.1 Trisine Wave Vector Multiples(KK) Compared To $K_B K_B$

		$\frac{(KK)e^{Euler}}{\pi \sinh(trisine)}$	
K	$\frac{(KK)}{K_B K_B}$	$\frac{(KK)}{K_B K_B} \frac{1}{e^{trisine} - 1}$	$\frac{K}{K_B}$
K_{D_n}	1.1981	0.1852	1.0946
K_P	1.3333	0.2061	1.1547
K_{D_s}	3.1132	0.4812	1.7644
K_C	3.3526	0.5182	1.8310
K_A	22.6300	3.4976	4.7571

APPENDIX B. DEBYE MODEL NORMAL AND TRISINE RECIPROCAL LATTICE WAVE VECTORS

This appendix parallels the presentation made in ref [4 pages 121 - 122].

$$N = \begin{bmatrix} \left(\frac{L}{2\pi}\right)^3 \frac{4\pi}{3} K_{Dn}^3 \\ \left(\frac{L}{2\pi}\right)^3 K_{Ds}^3 \end{bmatrix} = \begin{bmatrix} \text{Debye Spherical Condition} \\ \text{Debye Trisine Condition} \end{bmatrix} \quad (\text{B.1})$$

where:

$$K_{Ds} = (K_A K_B K_C)^{\frac{1}{3}} \quad (\text{B.2})$$

$$\frac{dN}{d\omega} = \begin{bmatrix} \frac{\text{cavity}}{2\pi^2} K_{Dn}^2 \frac{dK_{Dn}}{d\omega} \\ \frac{\text{cavity}}{8\pi^3} 3K_{Ds}^2 \frac{dK_{Ds}}{d\omega} \end{bmatrix} = \begin{bmatrix} \text{Debye Spherical Condition} \\ \text{Debye Trisine Condition} \end{bmatrix} \quad (\text{B.3})$$

$$K = \frac{\omega}{v} \quad (\text{B.4})$$

$$\frac{dK}{d\omega} = \frac{1}{v} \quad (\text{B.5})$$

$$\frac{dN}{d\omega} = \begin{bmatrix} \frac{\text{cavity}}{2\pi^2} \frac{\omega^2}{v^3} \\ \frac{3 \cdot \text{cavity}}{8\pi^3} \frac{\omega^2}{v^3} \end{bmatrix} = \begin{bmatrix} \text{Debye spherical} \\ \text{Debye trisine} \end{bmatrix} \quad (\text{B.6})$$

$$N = \begin{bmatrix} \frac{\text{cavity}}{6\pi^2} \frac{\omega^3}{v^3} \\ \frac{\text{cavity}}{8\pi^3} \frac{\omega^3}{v^3} \end{bmatrix} = \begin{bmatrix} \frac{\text{cavity}}{6\pi^2} K_{Dn}^3 \\ \frac{\text{cavity}}{8\pi^3} K_{Ds}^3 \end{bmatrix} = \begin{bmatrix} \text{Debye Spherical Condition} \\ \text{Debye Trisine Condition} \end{bmatrix} \quad (\text{B.7})$$

Given that $N = 1$ Cell

$$\begin{bmatrix} K_{Dn} \\ K_{Ds} \end{bmatrix} = \begin{bmatrix} \left(\frac{6\pi^2}{\text{cavity}}\right)^{\frac{1}{3}} \\ \left(\frac{8\pi^3}{\text{cavity}}\right)^{\frac{1}{3}} \end{bmatrix} = \begin{bmatrix} \text{Debye Spherical Condition} \\ \text{Debye Trisine Condition} \end{bmatrix} \quad (\text{B.8})$$

APPENDIX C. ONE DIMENSION AND TRISINE DENSITY OF STATES

This appendix parallels the presentation made in ref [4 pages 144-155].

Trisine

$$\frac{2K_c^3}{\left(\frac{2\pi}{L}\right)^3} = N \quad (\text{C.1})$$

One Dimension

$$\epsilon = \frac{\hbar^2}{2m_i} N^2 \frac{\pi^2}{(2B)^2} \quad (\text{C.2})$$

Now do a parallel development of trisine and one dimension density of states.

$$N = \begin{bmatrix} \frac{2K_c^3 \cdot \text{cavity}}{8\pi^3} \\ \left(\frac{2m_i}{\hbar^2}\right)^{\frac{1}{2}} \frac{2B}{\pi} \epsilon^{\frac{1}{2}} \end{bmatrix} = \begin{bmatrix} \text{Trisine Dimensional Condition} \\ \text{One Dimensional Condition} \end{bmatrix} \quad (\text{C.3})$$

$$\frac{dN}{d\epsilon} = \left[\begin{array}{l} \frac{2 \cdot \text{cavity} \left(\frac{2m_t}{\hbar^2} \right)^{\frac{3}{2}} \frac{3}{2} \epsilon^{\frac{1}{2}}}{8\pi^3} \\ \left(\frac{2m_t}{\hbar^2} \right)^{\frac{1}{2}} \frac{2B}{\pi} \frac{1}{2} \epsilon^{-\frac{1}{2}} \end{array} \right] = \left[\begin{array}{l} \text{Trisine} \\ \text{Dimensional} \\ \text{Condition} \\ \\ \text{One} \\ \text{Dimensional} \\ \text{Condition} \end{array} \right] \quad (\text{C.4})$$

$$\frac{dN}{d\epsilon} = \left[\begin{array}{l} \frac{2 \cdot \text{cavity} \left(\frac{2m_t}{\hbar^2} \right)^{\frac{3}{2}} \frac{3}{2} \epsilon^{\frac{1}{2}}}{8\pi^3} \\ \left(\frac{2m_t}{\hbar^2} \right)^{\frac{1}{2}} \frac{2B}{\pi} \frac{1}{2} \epsilon^{-\frac{1}{2}} \end{array} \right] = \left[\begin{array}{l} \text{Trisine} \\ \text{Dimensional} \\ \text{Condition} \\ \\ \text{One} \\ \text{Dimensional} \\ \text{Condition} \end{array} \right] \quad (\text{C.5})$$

$$\frac{dN}{d\epsilon} = \left[\begin{array}{l} 2 \frac{3}{2} \frac{\text{cavity}}{8\pi^3} \left(\frac{2m_t}{\hbar^2} \right)^{\frac{3}{2}} \left(\frac{2m_t}{\hbar^2} \right)^{-\frac{1}{2}} K_C \\ \left(\frac{2m_t}{\hbar^2} \right)^{\frac{1}{2}} \frac{2B}{\pi} \frac{1}{2} \left(\frac{2m_t}{\hbar^2} \right)^{\frac{1}{2}} \frac{1}{K_B} \end{array} \right] \quad (\text{C.6})$$

$$= \left[\begin{array}{l} \text{Trisine} \\ \text{Dimensional} \\ \text{Condition} \\ \\ \text{One} \\ \text{Dimensional} \\ \text{Condition} \end{array} \right]$$

$$\frac{dN}{d\epsilon} = D(\epsilon) = \left[\begin{array}{l} \frac{3}{8} \frac{\text{cavity}}{\pi^3} \left(\frac{2m_t}{\hbar^2} \right) K_C \\ \frac{2m_t}{\hbar^2 K_B^2} \end{array} \right] \quad (\text{C.7})$$

$$= \left[\begin{array}{l} \text{Trisine} \\ \text{Dimensional} \\ \text{Condition} \\ \\ \text{One} \\ \text{Dimensional} \\ \text{Condition} \end{array} \right]$$

Now equating trisine and one dimensional density of states results in equation C.8.

$$K_C = \frac{8\pi^3}{3 \cdot \text{cavity} \cdot K_B^2} \quad (\text{C.8})$$

$$= \frac{4\pi}{3\sqrt{3}A}$$

$\epsilon =$ energy
 $D(\epsilon) =$ density of states

APPENDIX D. GINZBURG-LANDAU EQUATION AND TRISINE STRUCTURE RELATIONSHIP

This appendix parallels the presentation made in ref [4 Appendix I].

$$|\psi|^2 = \frac{\alpha}{\beta} \quad (\text{D.1})$$

$$= \frac{\text{Cooper}}{\text{Cavity}}$$

$$\frac{\alpha^2}{2\beta} = \frac{k_b T_c}{\text{chain}} \quad (\text{D.2})$$

$$= \frac{\hbar^2 K_B^2}{2m_t \cdot \text{chain}}$$

$$= \frac{H_c^2}{8\pi}$$

$$\lambda = \frac{m_t v_\epsilon^2}{4\pi (\text{Cooper} \cdot e)^2 |\psi|^2} \quad (\text{D.3})$$

$$= \frac{m_t v_\epsilon^2 \beta}{4\pi q^2 \alpha}$$

$$= \frac{m_t v_\epsilon^2 \text{cavity}}{4\pi (\text{Cooper} \cdot e)^2 \text{Cooper}}$$

$$\beta = \frac{\alpha^2 2m_t \text{chain}}{2\hbar^2 K_B^2} \quad (\text{D.4})$$

$$= \frac{\alpha^2 \text{chain}}{2k_b T_c}$$

$$\begin{aligned}\alpha &= \beta \frac{\text{Cooper}}{\text{cavity}} & (D.5) \\ &= \frac{\alpha^2 2m_i \text{chain}}{2\hbar^2 K_B^2} \frac{\text{Cooper}}{\text{cavity}} \\ &= \frac{\alpha^2 \text{chain}}{2k_b T_c} \frac{\text{Cooper}}{\text{cavity}}\end{aligned}$$

$$\begin{aligned}\alpha &= k_b T_c \frac{\text{cavity}}{\text{chain}} & (D.6) \\ &= \frac{\hbar^2 K_B^2}{2m_i} \frac{\text{cavity}}{\text{chain}}\end{aligned}$$

$$\begin{aligned}\xi^2 &\equiv \frac{\hbar^2}{2m_e \alpha} & (D.7) \\ &= \frac{\hbar^2}{2m_e} \frac{2m_i \cdot \text{chain}}{\hbar^2 K_B^2 \cdot \text{cavity}} \\ &= \frac{m_i}{m_e} \frac{1}{K_B^2} \frac{\text{chain}}{\text{cavity}}\end{aligned}$$

$$\begin{aligned}H_{c2} &= \frac{\phi_\varepsilon \cdot 2 \cdot 4\pi}{\text{section}} & (D.8) \\ &= \frac{\phi_\varepsilon}{\pi \xi^2} \frac{m_i}{m_e} \frac{\text{cavity}}{\text{chain}}\end{aligned}$$

APPENDIX E. LORENTZ EINSTEIN TRANSFORMATION CONSEQUENCES

Given relativistic CPT times $_{\pm}(\Delta t^{\bullet})$ and (Δt) then define the Lorentz Einstein Transformation Consequence as:

$$\Delta t = \frac{\Delta t^{\bullet}}{\sqrt{1 - \frac{v^2}{c^2}}} \quad \text{and} \quad \frac{\Delta t^{\bullet}}{\Delta t} = \sqrt{1 - \frac{v^2}{c^2}} \quad (E.1)$$

then

$$1 - \frac{\Delta t^{\bullet}}{\Delta t} = \frac{\Delta t - \Delta t^{\bullet}}{\Delta t} = 1 - \sqrt{1 - \frac{v^2}{c^2}} \quad (E.2)$$

Then

$$\Delta t = \frac{\Delta t - \Delta t^{\bullet}}{1 - \sqrt{1 - \frac{v^2}{c^2}}} \quad (E.3)$$

$$\text{and } \Delta t = 2(\Delta t - \Delta t^{\bullet}) \frac{c^2}{v^2}$$

where $v \ll c$

Given relativistic lengths (Δl^{\bullet}) and (Δl) then define the Lorentz Einstein Transformation Consequence as:

$$\Delta l^{\bullet} = \frac{\Delta l}{\sqrt{1 - \frac{v^2}{c^2}}} \quad \text{and} \quad \frac{\Delta l}{\Delta l^{\bullet}} = \sqrt{1 - \frac{v^2}{c^2}} \quad (E.4)$$

then

$$1 - \frac{\Delta l}{\Delta l^{\bullet}} = \frac{\Delta l^{\bullet} - \Delta l}{\Delta l^{\bullet}} = 1 - \sqrt{1 - \frac{v^2}{c^2}} \quad (E.5)$$

then

$$\Delta l^{\bullet} = \frac{\Delta l^{\bullet} - \Delta l}{1 - \sqrt{1 - \frac{v^2}{c^2}}} \quad (E.6)$$

$$\text{and } \Delta l^{\bullet} = 2(\Delta l^{\bullet} - \Delta l) \frac{c^2}{v^2} \quad \text{where } v \ll c$$

Given relativistic masses (Δm^{\bullet}) and (Δm) then define the Lorentz Einstein Einstein Transformation Consequence as:

$$\Delta m^{\bullet} = \frac{\Delta m}{\sqrt{1 - \frac{v^2}{c^2}}} \quad \text{and} \quad \frac{\Delta m}{\Delta m^{\bullet}} = \sqrt{1 - \frac{v^2}{c^2}} \quad (E.7)$$

then

$$1 - \frac{\Delta m}{\Delta m^{\bullet}} = \frac{\Delta m^{\bullet} - \Delta m}{\Delta m^{\bullet}} = 1 - \sqrt{1 - \frac{v^2}{c^2}} \quad (E.8)$$

then

$$\Delta m^{\bullet} = \frac{\Delta m^{\bullet} - \Delta m}{1 - \sqrt{1 - \frac{v^2}{c^2}}} \quad (E.9)$$

$$\text{and } \Delta m^{\bullet} = 2(\Delta m^{\bullet} - \Delta m) \frac{c^2}{v^2}$$

where $v \ll c$

6. REFERENCES

- [1] William Melis and Richard Saam, "U. S. Patent 4,526,691", Separator Apparatus, July 2, 1985.
- [2] J. Bardeen, L. N. Cooper and J. R. Schrieffer, "Theory of Superconductivity", Physical Review, Vol 28, Number 6, December 1, 1957, pages 1175-1204.
- [3] E. Schrödinger, "An Undulatory Theory of the Mechanics of Atoms and Molecules", Physical Review, Vol 108, Number 5, December, 1926, pages 1049-1069.
- [4] Charles Kittel, Introduction to Solid State Physics, Seventh Edition, John Wiley & Sons, Inc., New York, N.Y., 1996.
- [5] W. A. Little, "Experimental Constraints on Theories of High Transition Temperature Superconductors", Department of Applied Physics, Stanford University, 1987.
- [6] Leonard Eyges, "The Classical Electromagnetic Field", Dover Edition, New York, New York, 1980.
- [7] E. Podkletnov and R. Nieminen, "A Possibility of Gravitational Force Shielding by Bulk $YBa_2Cu_2O_{7-x}$ Superconductor", Physica C 203, (1992), 414-444.
- [8] Sir Arthur Eddington, "The Universe and the Atom" from The Expanding Universe, Cambridge University Press.
- [9] Giovanni Modanese, "Theoretical Analysis of a Reported Weak Gravitational Shielding Effect", MPI-PhT/95-44, May 1995, Max-Planck-Institut für Physik, Werner-Heisenberg-Institut, Föhringer Ring 6, D 80805 München (Germany) to appear in Europhysical Letters.
- [10] Giovanni Modanese, "Role of a 'Local' Cosmological Constant in Euclidian Quantum Gravity", UTF-368/96 Jan 1996, Gruppo Collegato di Trento, Dipartimento di Fisica dell'Universita I-38050 POVO (TN) - Italy
- [11] J. E. Sonier et al, "Magnetic Field Dependence of the London Penetration Depth in the Vortex State of $YBa_2Cu_2O_{6.95}$ ", Triumpf, Canadian Institute for Advanced Research and Department of Physics, University of British Columbia, Vancouver, British Columbia, Canada, V6T.
- [12] T. R. Camp and P. C. Stein, "Velocity Gradients and Internal Work in Fluid Motion", J. Boston Soc. Civil Engrs., 30, 219 (1943).
- [13] Miron Smoluchowski, Drei Vorträge über Diffusion, Brownsche Molekularbewegung und Koagulation von Kolloidteilchen (Three Lectures on Diffusion, Brownian Motion, and Coagulation of Colloidal Particles), Phys. Z., 17, 557 (1916); Versuch einer Mathematischen Theorie der Koagulationskinetik Kolloider Lösugen (Trial of a Mathematical Theory of the Coagulation Kinetics of Colloidal Solutions), Z. Physik. Chem., 92, 129, 155 (1917).
- [14] Fair, Geyer and Okun, Water and Wastewater Engineering, John Wiley & Sons, Inc. New York, 1968, pages 22-9 to 22-14.
- [15] Georg Joos, Theoretical Physics, translated from the first German Edition by Ira Freeman, Hafner Publishing Company, Inc., New York 1934.
- [16] R. Weast, Handbook of Chemistry and Physics, 53 Edition, The Chemical Rubber Company, Cleveland, Ohio, 1972-73.
- [17] D. R. Harshman and A. P. Mills, Jr., "Concerning the Nature of High-Tc Superconductivity: Survey of Experimental Properties and Implications for interlayer Coupling", Physical Review B, 45,18,1May 92.
- [18] J. Vennard, Fluid Mechanics, John Wiley & Sons, Inc., New York, NY, 1961.
- [19] W. Moore, Physical Chemistry, Prentice-Hall, Inc., Englewood Cliffs, NJ, 1962.
- [20] Takeshi Fukuyama, "Late-Time Mild Inflation-a possible solution of dilemma: cosmic age and the Hubble parameter", Department of Physics, Ritsumeikan University, Kusatsu Shiga, 525-77 JAPAN, August 14, 1996.
- [21] Hayasaka and Takeuchi, "Anomalous Weight Reduction on a Gyroscope's Right Rotations around the Vertical Axis on the Earth", Physical Review Letters, 63, 25, December 18, 1989, p 2701-4.
- [22] Faller, Hollander, and McHugh, "Gyroscope-Weighing

- Experiment with a Null Result", *Physical Review Letters*, 64, 8, February 19, 1990, p 825-6.
- [23] Nitschke and Wilmarth, "Null Result for the Weight Change of a Spinning Gyroscope", *Physical Review Letters*, 64, 18, April 30, 1990, p 2115-16.
- [24] Cram and Hammond, *Organic Chemistry*, McGraw-Hill Book Company, New York, NY 1964.
- [25] Kimberly, Chanmugan, Johnson, & Tohline, Millisecond Pulsars Detectable Sources of Continuous Gravitational Waves, *Astrophysics J.*, 450:757, 1995.
- [26] Staggs, Jarosik, Meyer and Wilkinson, Enrico Fermi Institute, University of Chicago, Chicago, Illinois 60637, Sept 18, 1996.
- [27] Copi, Schramm and Turner, *Science*, 267, January 13, 1995, pp 192-8.
- [28] Albert Einstein, *The Meaning of Relativity, Fifth Edition*, MJF Books, New York, NY 1956.
- [29] Albert Einstein, *The Special and the General Theory*, Three Rivers Press, New York, NY 1961.
- [30] Wolfgang Pauli, *The Theory of Relativity*, Dover Publications, New York, NY 1958.
- [31] Robert M. Wald, *General Relativity*, University of Chicago Press, Chicago, 1984.
- [32] Ray D'Inverno, *Introducing Einstein's Relativity*, Clarendon Press, Oxford, 1995.
- [33] Paul A. M. Dirac, *General Theory of Relativity*, Princeton University Press, Princeton, NJ, 1996.
- [34] Barrett O'Neill, *The Geometry of Kerr Black Holes*, A K Peters, Wellesley, MA, 1995.
- [35] Charles W. Misner, Kip S. Thorne & John A. Wheeler, *Gravitation*, W. H. Freeman and Company, New York, 1998.
- [36] Rutherford Aris, *Vectors, Tensors, and the Basic Equations of Fluid Mechanics*, Dover Publications, New York, 1962.
- [37] Heinrich W. Guggenheimer, *Differential Geometry*, Dover Publications, New York, 1977.
- [38] Hans Schneider, George P. Barker, *Matrices and Linear Algebra*, Dover Publications, New York, 1962.
- [39] Bernard Schutz, *Geometrical Methods of Mathematical Physics*, Cambridge University Press, Cambridge, 1980.
- [40] Richard P. Feynman, *Six Easy Pieces*, Addison-Wesley Publishing Company, New York, 1995.
- [41] Jed Z. Buchwald, *From Maxwell to Microphysics*, University of Chicago Press, Chicago, 1973.
- [42] Thomas K. Simpson, *Maxwell on the Electromagnetic Field*, Rutgers University Press, New Brunswick, NJ, 1997.
- [42] Leonard Eyges, *The Classical Electromagnetic Field*, Dover Publications, New York, 1972.
- [43] L. D. Landau and E. M. Lifshitz, *The Classical Theory of Fields, Volume 2*, Butterworth-Heinenann, Oxford, 1998.
- [44] C. K. Birdsall & A. B. Langdon, *Plasma Physics via Computer Simulation*, Institute of Physics Publishing, Philadelphia, 1991.
- [45] Peter W. Milonni, *The Quantum Vacuum, An Introduction to Quantum Electrodynamics*, Academic Press, New York, 1994.
- [46] Claude Cohen-Tannoudju, Jacques Dupont-Roc & Gilbert Grynberg, *Photons & Atoms, Introduction to Quantum Electrodynamics*, John Wiley & Sons, Inc., New York, 1989.
- [47] Eugen Merzbacher, *Quantum Mechanics, Third Edition*, John Wiley & Sons, Inc., New York, 1998.
- [48] James P. Runt and John J. Fitzgerald, *Dielectric Spectroscopy of Polymeric Materials, Fundamentals and Applications*, American Chemical Society, Washington, DC, 1997.
- [49] Michael Tinkham, *Introduction to Superconductivity*, McGraw-Hill Companies, New York, NY, 1996.
- [50] Eugene Hecht, *Optics Third Edition*, Addison-Wesley,

- New York, NY, 1998.
- [51] C. C. Homes et al, Universal Scaling Relation in High-Temperature Superconductors. *Nature*, Vol 430, 29 July 2004.
<http://xxx.lanl.gov/abs/cond-mat/0404216>
- [52] Jan Zaanen, Why the Temperature is High, *Nature*, Vol 430, 29 July 2004.
- [53] Study of the anomalous acceleration of Pioneer 10 and 11, John D. Anderson, Philip A. Laing, Eunice L. Lau, Anthony S. Liu, Michael Martin Nieto, and Slava G. Turyshev, July 9, 2004
<http://arxiv.org/abs/gr-qc/0104064>
- [54] C. C. Homes et al, Are high-temperature superconductors in the dirty limit.
<http://xxx.lanl.gov/abs/cond-mat/0410719>
- [55] N. Klein, B.B. Jin, J. Schubert, M. Schuster, H.R. Yi, Forschungszentrum Jülich, Institute of Thin Films and Interfaces, D-52425 Jülich, Germany, A. Pimenov, A. Loidl, Universität Augsburg, Experimentalphysik V, EKM, 86135 Augsburg, Germany, S.I. Krasnosvobodtsev, P.N. Lebedev Physics Institute, Russian Academy of Sciences, 117924 Moscow, Russia,
<http://xxx.lanl.gov/abs/cond-mat/0107259>, Energy gap and London penetration depth of MgB₂ films determined by microwave resonator, Submitted to *Physical Review Letters*, June 29, 2001. MgB₂ superconductivity originally discovered by Nagamatsu et al. 2001 Superconductivity at 39 K in magnesium diboride *Nature* 410 63
- [56] Directly Measured Limit on the Interplanetary Matter Density from Pioneer 10 and 11 Michael Martin Nieto, Slava G. Turyshev, and John D. Anderson
<http://arxiv.org/abs/astro-ph/0501626>
- [57] Study of the Pioneer Anomaly: A Problem Set, Slava G. Turyshev, Michael Martin Nieto, and John D. Anderson <http://arxiv.org/abs/astro-ph/0502123>
- [58] Heliocentric Trajectories for Selected Spacecraft, Planets, and Comets, NSSDC Goddard National Spaceflight Center, <http://nssdc.gsfc.nasa.gov/space/helios/heli.html>
- [59] Scaling of the superfluid density in high-temperature superconductors Authors: C. C. Homes, S. V. Dordevic, T. Valla, M. Strongin
<http://xxx.lanl.gov/abs/cond-mat/0410719>
- [60] Frank M. White, *Viscous Fluid Flow*, Second Edition, McGraw Hill. NY, NY, 1974
- [61] F. W. Sears, M. W. Zemansky, *University Physics*, Third Edition, Addison-Wesley. Reading, MA, 1964
- [62] James L. Anderson, *Thompson Scattering in an Expanding Universe*,
<http://xxx.lanl.gov/abs/gr-qc/9709034>
- [63] Michael Martin Nieto, Slava G. Turyshev, *Measuring the Interplanetary Medium with a Solar Sail*,
<http://xxx.lanl.gov/abs/gr-qc/0308108>

Acknowledgements: Jiri Kucera, Joseph Krueger,
Chris Tolmie, William Rieken,
Alan Schwartz